Journal of Medicinal Chemistry

Article

Convergent Synthesis of Novel Muramyl Dipeptide Analogs: Inhibition of Porphyromonas gingivalis-induced Pro-inflammatory Effects by High Doses of Muramyl Dipeptide

Bin Cai, James S. Panek, and Salomon Amar

J. Med. Chem., **Just Accepted Manuscript** • DOI: 10.1021/acs.jmedchem.6b00681 • Publication Date (Web): 29 Jun 2016

ACS Publications

Journal of Medicinal Chemistry is published by the American Chemical Society. 1155 Sixteenth Street N.W., Washington, DC 20036

Convergent Synthesis of Novel Muramyl Dipeptide Analogs: Inhibition of Porphyromonas gingivalis-induced Pro-inflammatory Effects by High Doses of Muramyl Dipeptide

Bin Cai[§], James S. Panek[§] and Salomon Amar[†*]*

[†]Center for Anti-Inflammatory Therapeutics, Department of Molecular & Cell Biology, Boston University Goldman School of Dental Medicine, 650 Albany Street, Boston, MA, 02118

[§] Department of Chemistry, Boston University, Metcalf Center for Science and Engineering, 590 Commonwealth Avenue, Boston, MA, 02215

ABSTRACT

Porphyromonas gingivalis (P.g)-induced TNF-α can be affected by muramyl dipeptide (MDP) in a bi-phasic concentration-dependent manner. We found that in *P.g*-exposed macrophages, treatment with 10 μg/ml of MDP (MDP-low) up-regulated TNF-α by 29%, while 100 μg/ml or higher (MDP-high) significantly decreased it (16% to 38%). MDP-high was found to affect the ubiquitin-editing enzyme A20 and activator protein 1 (AP1). An AP1 binding site was found in the promoter region of A20. A20 promoter activity was up-regulated after transfection of AP1 cDNA in cells. Four analogs of MDP (**3**-**6**) were prepared through a convergent strategy involving the synthesis of two unique carbohydrate fragments, **7a** and **7b** using the peptide coupling reagents, EDCI and HOAt. Analog **4** improved MDP function and *P.g*-induced activities. We propose a new signaling pathway for TNF-α induction activated after exposing macrophages to both *P.g* and MDP-high or analog **4**.

1) INTRODUCTION

Two major classes of pattern recognition receptors (PRRs) include membrane-bound Toll-like receptors (TLRs) and soluble, cytosolic nucleotide-binding oligomerization domain (NOD) like receptors (NLRs)[1]. Where TLRs help to sense extracellular pathogens, NLRs provide surveillance of the cytosol. Mammals have two closely related NOD family members, NOD1 and NOD2, both of which contain caspase recruitment domains (CARDs), a central NOD (NACHT) domain, and C-terminal Leu-rich repeats (LRRs)[2-5]. Studies have linked NOD2 mutations to severe inflammatory diseases[6-7], suggesting that NOD2 might play a pathophysiological role in inflammatory disorders. However it is important to note that chronic stimulation of NOD2 was reported to mediate tolerance to bacterial products.[6-7] The mechanism(s) behind this tolerance remain poorly understood. Following breakdown of bacterial cell walls, muramyl dipeptide (MDP) is formed and detected by NOD2. Upon detection of low doses of MDP, NOD2 binds to the kinase receptor-interacting protein 2 (RIP2) via CARD-CARD homophilic interactions—a necessary step for downstream signaling to proceed.[8-10] Signaling to RIP2 leads to NFκB transcriptional activity through the inhibitor of κB (IκB) kinase complex, as well as other cascades involving mitogen-activated protein (MAP) kinases that result in the production of pro-inflammatory cytokines and chemokines such as interleukin-6 (IL-6), TNF-α, IL-12, and IL-8[11]. In contrast, a higher dose of MDP has been found to dampen the inflammatory response[12-13]. Studies on NOD2 mutations suggest that NOD2 might mediate tolerance to bacterial products, but the precise mechanisms have not yet been identified.[6,14]

The effects of MDP are biphasic: at 10 μg/ml (MDP-low), MDP activates the inflammatory process, while a dose of 100 μg/ml or higher (MDP-high) dampens the process by inhibiting the NFkB-mediated cytokine response.[7,15-16] No signs of cytotoxicity or apoptosis were observed *in*

vitro at high MDP doses[15]. While the pro-inflammatory effects of low doses of MDP are well documented, the mechanisms behind the anti-inflammatory effects of high doses of MDP remain unclear. Understanding the dual actions of MDP on NOD2 may reveal an important signaling pathway that may be therapeutically important in chronic inflammatory conditions.

The realization that MDP and its derivatives exhibit potent anti-inflammatory effects has resulted in active research programs in both academia[17] and industries. Mifamurtide, an analog of MDP originally developed by Novartis and commercialized by Takeda, was approved in the United States and Europe for the treatment of osteosarcoma. In reviewing studies aimed at identifying pro-inflammatory cytokine inhibitors, we learned that conformationally biased (bicyclic systems) MDP derivatives serve as new lead compounds accessed through an efficient convergent synthesis. A literature search revealed that existing methods did not describe the preparation of conformationally biased, bicyclic analogs[18-21] which are the first examples of this therapeutic class. In addition, few reports[19-20,22-25] have fully characterized synthetic intermediates and final products, while also allowing for their preparation in quantities that would be sufficient for biological evaluation[18-20,26] (see Supporting Information for details). This work enables the production of stereochemically pure compounds in useful quantities: >20 grams of the *N*-acetyl sugar fragment in a four-step sequence, requiring a single purification step and features an efficient, seven-step route to the associated dipeptides.

With this chemical strategy in place, we looked for the signal transduction pathway associated with the biochemical effects of MDP-high on inflammation. Based on previous studies showing that the ubiquitin-editing enzyme A20 functions as an anti-inflammatory protein[27] and as a key negative regulator of NFκB, [28] we proposed a role of A20 in MDP anti-inflammatory function.

Four enantiomerically enriched analogs of MDP were synthesized and among them, analog **4** exhibited the most potent activity. A new signaling pathway mediated by MDP-high or analog **4** after *Porphyromonas gingivalis (P.g)* stimulation is hereto advocated.

2) RESULTS AND DISCUSSION

2.1) MDP effects on *P.g*-induced TNF-α, A20, and other factors

Our previous data indicated that LPS-induced TNF-α in macrophages was increased by concurrent treatment with MDP-low treatment but surprisingly, was decreased by MDP-high treatment[7 29]. To further confirm this, a dose course of MDP was performed. As shown in Figure 1, MDP-low up-regulated *P.g*-induced TNF-α by 29% but MDP-high significantly decreased *P.g*-induced TNF-α secretion by 16% to 38% in macrophages. Furthermore, in order to see whether a higher dose of MDP had an immediate toxic effect on cell survival, a toxicity test was performed. As shown in Figure 2, neither the low nor high-dose MDP treatments significantly affected macrophage survival, even when a much higher dose (1,000 μg/ml) of MDP was used. Meanwhile, we also found that a high dose of MDP in macrophages did not affect NOD2 or RIP2 transcription (Figure 3A-D). However, this treatment significantly induced A20 with a 5.6-fold increase in mRNA levels, as compared to the control, while MDP-low treatment did not (Figure 3E). This phenomenon was further confirmed by Western blot analysis (Figure 4). Interestingly, we also found that this treatment up-regulated the activator protein 1 (AP1) production but not MyD88, NFκB (Figure 4A), p53, or p21 (Figure 4B), compared to the control.

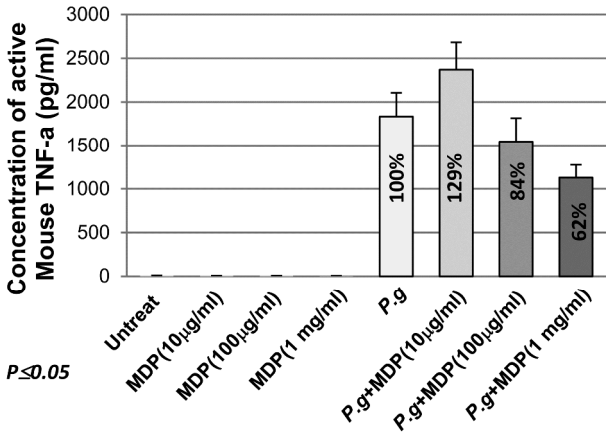

Figure 1. ELISA analysis of TNF-α expression. The pre-cultured primary macrophages from wild-type (WT) mice were untreated or treated with 10, 100, 1,000 μg/ml of MDP as the control, or treated with P.g alone as a positive control, or co-treated with P.g plus 10, 100, or 1,000 μg/ml of MDP for 3 h. The media from each test group were used to detect TNF-α via an ELISA kit (Invitrogen). Data are represented as Mean ±S.E. *p≤0.05.

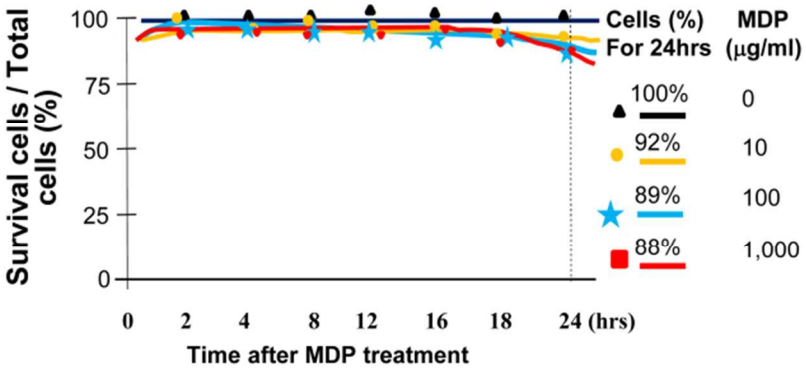

Figure 2. Toxicity test. WT mouse macrophages were treated with different quantities of MDP for 0, 2, 4, 8, 12, 16, 18, 24 h. Cells from each time point were collected by Trypsin. Cells were stained by Trypan blue and their survival rate was calculated. The survival rate by 0 μg/ml of MDP for 24 h was assigned a value of 100% as the baseline, to which the actual values of the others was compared. Data are represented as Mean ±S.E. *p≤0.05.

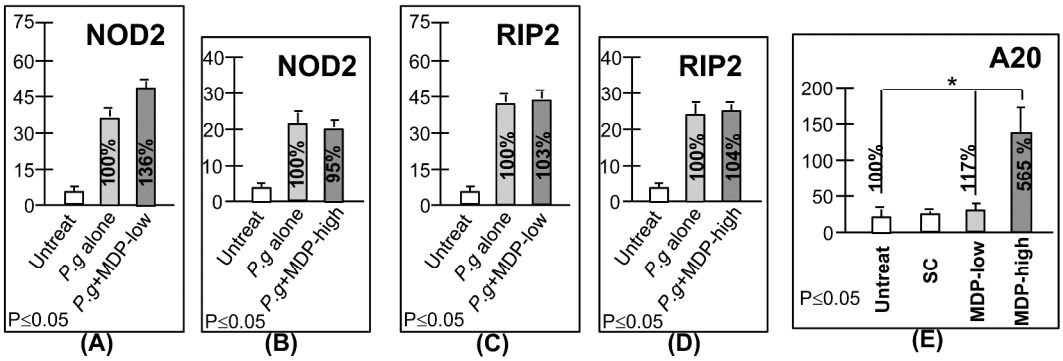

Figure 3. RT-PCR analysis of MDP-mediated gene expression. WT mouse macrophages were untreated as the negative control, *P.g* alone as the positive control, or co-treated with *P.g* plus MDP-low treatment, or MDP-high treatment for 3 h. Total mRNA from each test group were assessed by RT-PCR with the primers of NOD2, RIP2, or A20 and normalized with GAPDH. The intensity of mRNA levels of NOD2, or RIP2 from the *P.g* alone treatment (**A-D**) were assigned to a base value (100%). For A20, the intensity of mRNA levels after MDP-low treatment (**E**) was assigned to a base value (100%). The others were calculated relative to this base value. Triplicate assays were conducted. Mean SEM.

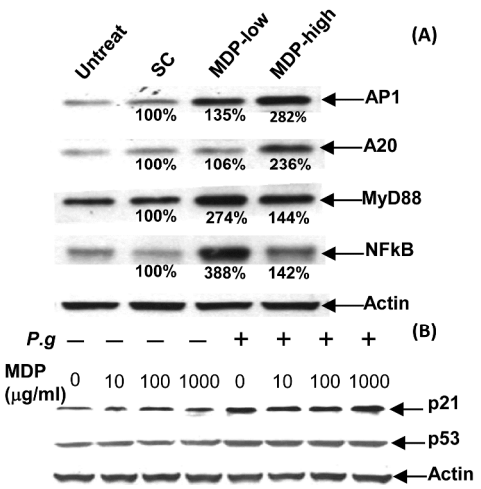

Figure 4. Western blot analysis. WT mouse macrophages were untreated or treated with a SC peptide as the negative control, MDP-low treatment, or MDP-high treatment for 3 h. The total protein from each test group was assessed by Western blot with antibodies (Abs) acting against AP1, A20, MyD88, NFkB, or Actin as the control. The intensity of protein levels by treatment of a SC peptide was assigned a value of 100% as the baseline, to which the actual value of others was compared (**A**). WT mouse macrophages were treated with either different doses of MDP (0, 10, 100, 1,000 μg/ml), or co-treated with *P.g* plus different doses of MDP (0, 10, 100, 1,000 μg/ml) for 3 h. The total protein from each test group was assessed by Western blot with Abs against p21, p53, or Actin as the control (**B**). Triplicate assays are presented.

2.2) Activation of A20 via AP1 protein/DNA interaction

Because MDP-high treatment in cells induced both A20 and AP1, we hypothesize that they are associated in the response to MDP. Through further analysis of the A20 DNA sequence, we found that the promoter region of A20 contains an AP1 binding site (Figure 5A). In order to determine whether AP1 interacts with A20, a ChIP analysis assay using RAW 264.7 cells was performed. As shown in Figure 5B, a PCR amplification of the A20 promoter DNA was observed when cells were treated with MDP-high but not MDP-low, compared to the control (transfected with AP1 cDNA). To determine the region of the A20 promoter important for AP1 binding activity, RAW 264.7 cells were co-transfected with A20 promoter DNA and different concentrations of AP1 cDNA, after which the protein from each test group was assessed via a luciferase assay. As shown in Figure 6, A20 promoter activity increased dose-dependently with increasing AP1 cDNA concentration, indicating that AP1 is an important factor for up-regulating A20 via protein/DNA interactions. As it is well known that activation of A20 restricts NOD2,[30-31] we therefore propose a new signaling pathway mediated by high doses of MDP treatment in

response to *P.g* (Figure 7). Specifically, we suggest that through this pathway, when cells are treated with a high dose of MDP, MDP is transferred into the cytoplasm and activates Jun *N*-terminal kinases (JNKs);[7] JNKs then up-regulate AP1, which in turn activates A20 and restricts NOD2 ubiquitination, consequently inhibiting TNF-α secretion that would otherwise have been induced in response to *P.g*. We speculate that the signal transduction pathway identified for MDP-high would be the same as the one activated by analog **4**.

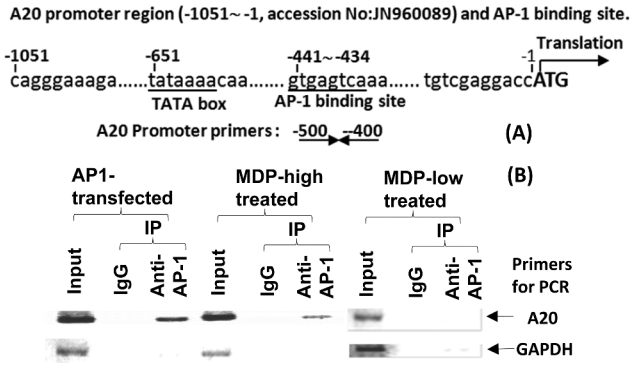

Figure 5. Chromatin Immunoprecipitation (ChIP) assay. Diagram of the A20 promoter region sequences, with the location of the AP1 binding site and PCR primers of A20 (**A**). DNA fragments of A20 or GAPDH as controls were amplified by PCR, with Input or IPs after the transfection of a full length AP1 cDNA in RAW264.7 cells (**B**). The assays were performed in triplicate and a representative experiment is presented.

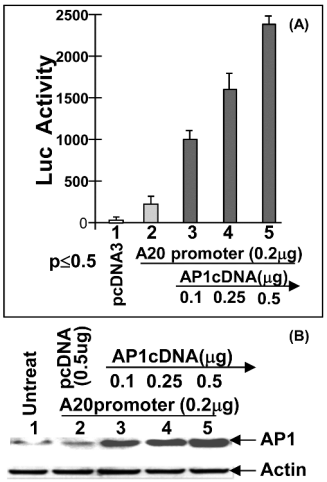

Figure 6. Promoter assay. RAW264.7 cells were transfected with pcDN3 (lane 1), 0.2 μg of the A20 promoter DNA alone (lane 2) as the control, co-transfected with the A20 promoter DNA (0.2 μg) plus different quantities of the full length AP1 cDNA (0.1 μg in lane 3, 0.25 μg in lane 4, 0.5 μg in lane 5). Proteins extracted from each group were measured by luciferase assay **(A)** and by Western blot **(B)**, with antibodies acting against AP1 or Actin as the control. Triplicate assays are presented.

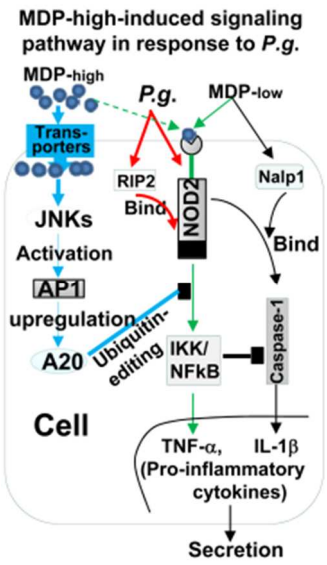

Figure 7. MDP-high-induced signaling pathway in response to *P.g*. MDP will be transferred into the cell's' cytoplasm and will activate JNKs, which will up-regulate AP1. AP1 will activate A20 and restrict NOD2 ubiquitin, consequently inhibiting TNF-α secretion in response to *P.g*.

2.3) Synthesis of novel MDP analogs

Since the discovery of the key role of MDP in NOD2-mediated innate immune responses to bacterial invasions in certain inflammatory diseases, research on the mechanism of actions and signaling pathways have been flourishing.[17,32-37] More recently, we have shown that treatment with higher concentration of MDP could have anti-inflammatory effects through regulating NOD2, mitigating atherosclerosis and bone loss. In a related study, the Kobayashi group[38] studied four MDP analogs and identified one aminosaccharide compound (DFK1012) which could inhibit the production of pro-inflammatory cytokines upon stimulation of the immune receptor proteins, TLR and/or NLR. DFK1012 has also proved to have no cytotoxicity, thus exhibiting promising anti-inflammatory effects. Since then, there have surprisingly been no further reports on the SAR of MDP pertaining to its anti-inflammatory effects. This underdeveloped, yet promising field prompted us to study the SAR of selected MDP analogs by employing a convergent synthesis strategy delineating the signaling pathway to analogs, and the

eventual identification of a lead compound. In that context, we targeted four novel analogs (Figure 8) because of their synthetic accessibility.

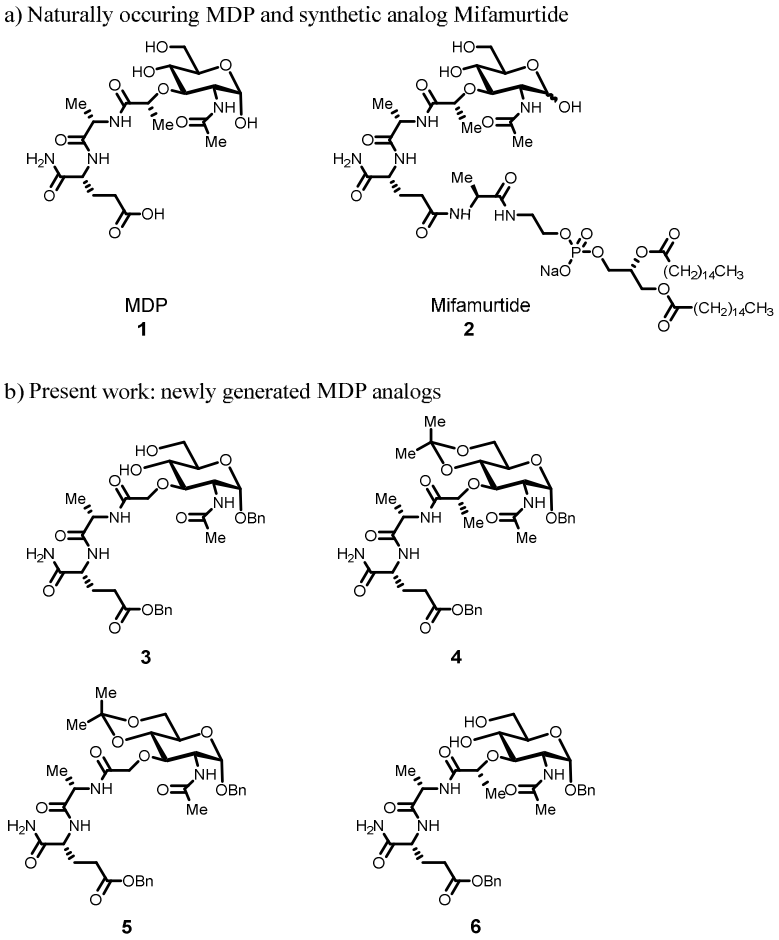

Figure 8. MDP and synthetic analogs of MDP

The underlying principles that guided us to design an early stage probe into the SAR were that the analogs (1) needed to be synthetically accessible, (2) must bear the features of both MDP and DFK1012, (3) and yet be differentiated from each other in subtle substitutions in the carbohydrate fragments. As such, we selected to independently modify the dipeptide and carbohydrate fragments before merging the two. In that regard, two variables were considered: the stereocenter on the lactic acid moiety and the rigidity the *N*-acetylmuramic acid fragment by incorporation of the cyclic ketal on the C4 and C6 hydroxyl groups, with the expectation that a conformationally biased carbohydrate fragment may provide guidance for further structural

optimization. As in Figure 8, analog **3** is devoid of the methyl-bearing stereocenter on the lactic acid subunit, while analog **6** contains the natural stereochemistry of the lactic acid moiety. Similarly, analog **5** was produced with the cyclic ketal and lastly, analog **4** merged the two variables—the (4*R*)-stereocenter of the lactic acid group and the bicyclic ketal.

Scheme 1. Retrosynthetic analysis of MDP analogs

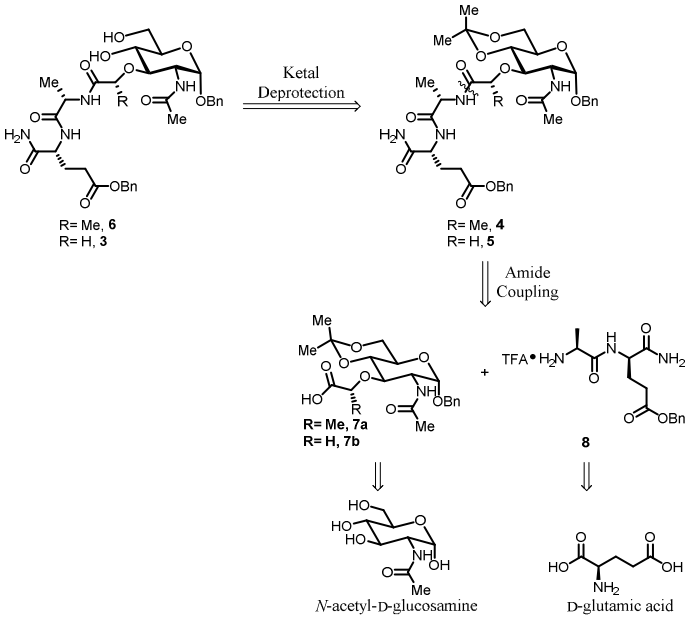

In our initial efforts toward the synthesis of MDP analogs, progress was hampered by low yielding reactions.[23-24,39-40] More importantly, these methods didn't allow for the preparation of the dipeptide fragment from simple, inexpensive, and/or commercially available materials. In that context, the Grimes group[26] described a synthetic approach leading to MDP-like agents that cleverly employed the functional group interconversion strategy of an azide to *N*-acylated variants at the C2-position, and subsequently studied their effects on NOD2 signaling and stability. The limitations of their synthesis include the production of mixtures of α/β-anomers of the carbohydrate fragments, and the inefficient route to the dipeptide.

Our approach focused on establishing a reliable, scalable, and divergent solution-phase synthesis of diastereomerically and enantiomerically pure MDP analogs in order to allow for the

preparation of MDP analogs in useful quantities for evaluating *P.g*-induced pro-inflammatory cytokine inhibitors. The present work marks the first reliable preparation of this dipeptide structural type with complete spectroscopic characterization of all intermediates and final products (see Supporting Information for details). In addition, the synthesis of carbohydrate fragments produced *N*-acetyl glucosamine scaffolds as single α-anomers.[22,41] Retrosynthetically, analogs **6** and **3** could be derived respectively through removal of the ketal of **4** and **5** (Scheme 1). Analogs **4** and **5** could be constructed by standard peptide coupling between carboxylic acids **7a** and **7b** and dipeptide **8**, which were synthesized respectively from commercially available *N*-acetyl-D-glucosamine and D-glutamic acid.

Scheme 2. Synthesis of carboxylic acids **7a** and **7b**[a]

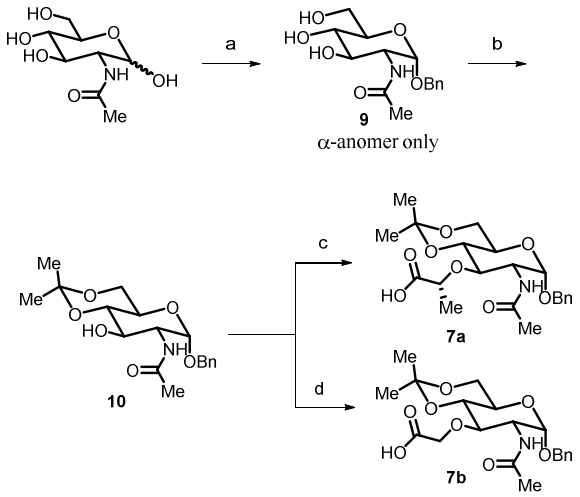

[a]Reagents and conditions: (a) Benzyl alcohol, HCl, 95 ºC, 4h, 64%; (b) 2,2-dimethoxypropane, *p*-TSA, acetone, r.t., 12h, 100%; (c) (*S*)-2-chloropropanoic acid, NaH, THF, 50ºC, 12h, 85%; (d) Bromoacetic acid, NaH, THF, 50ºC, 24h, 84%.

The synthesis of the carboxylic acids **7a** and **7b** commenced with the introduction of the benzyl ether at the anomeric position of *N*-acetyl-D-glucosamine (Scheme 2). Originally, we adopted a two-step sequence similar to that reported by Hecker et al.,[22] wherein the *N*-acetyl amino sugar **10** was produced by using intermediate **9** without purification. However, in our hands, we opted to purify **9** by recrystallizing it in hot ethanol before moving on to the next steps

and obtained **9** as a single α-anomer.[42] Thus, **9** was produced by heating *N*-acetyl-D-glucosamine in benzyl alcohol at 95°C, in the presence of anhydrous hydrochloric acid (1.0 equiv, 4N solution in 1,4-dioxane) in tetrahydrofuran (THF) as the promoter.[22] The orientation of the benzyl ether was assigned as axial based on the coupling constant J=3.5 Hz at δ=4.68 (characteristic of a *cis* axial-equatorial orientation) for the anomeric proton. The stereochemical assignment was further confirmed by Heteronuclear Single Quantum Coherence (HSQC) and Heteronuclear Multiple Bond Correlation (HMBC) nuclear magnetic resonance spectroscopic experiments (see Supporting Information for details). Protection of **9** with 2,2-dimethoxypropane and a catalytic amount of *p*-toluenesulfonic acid monohydrate (*p*-TsOH) in acetone afforded acetonide **10** with 100% conversion,[22] which was then used without further purification. O-alkylation of **10** with (*S*)-2-chloropropanoic acid[22] and bromoacetic acid using sodium hydride (3 equiv and 4 equiv, respectively) as a base in THF cleanly produced alkylation products **7a** and **7b** respectively. The production of **7a** as a single diastereomer was confirmed by comparing optical rotation of **7a** to the literature value ($[\alpha]_D^{24}$ = +118 (*c* 1.0, $CHCl_3$), literature $[\alpha]_D^{25}$ = +117 (*c* 1.0, $CHCl_3$).[22] Notably, this three-step sequence required only one single purification step employing a conventional chromatography on SiO_2 (silica gel). Accordingly, we established a facile and scalable route that allowed for the preparation of the functionalized glucosamines **7a** and **7b** in multi-gram quantities (>20 grams) with an overall yield of 43% (see Supporting Information for details).

The preparation of dipeptide **17** was guided by a desire to establish a reproducible route suitable for multi-gram production of the diastereomerically and enantiomerically pure material (Scheme 3). A disconnection at the peptide bond revealed that the dipeptide could be constructed by peptide coupling between the trifluoroacetic acid (TFA) salt of isoglutamine benzyl ester **16**

and Boc-L-alanine. Despite the fact that amino acid **16** is a substructure of the proposed MDP analogs, existing routes do not permit a gram-scale synthesis, and thus present an opportunity for further development.[23,25-26] In that regard, our synthesis commenced with a modified three-step sequence originally reported by Ressler.[25] Commercially available D-glutamic acid was protected as benzyl carbamate **11,** according to a published report by Abell[43], wherein the pH was carefully maintained in the range of 8 to 10 by using a combination of sodium carbonate and sodium bicarbonate in a solution of acetone and water (1:10). This crucial pH range minimized the decomposition of benzylchloroformate in an aqueous solution and prevented racemization of the derived carbamate. In our hands, the largest scale of this reaction in one pot was 10 grams with an excellent yield of 92%. It was postulated that the α-carboxylic acid of the bis-carboxylic acid **11** would exhibit a greater acidity than the γ-carboxylic acid, as evidenced by a smaller chemical shift of the α-carbon in the ^{13}C-NMR. Based on this assumption, a regioselective amidation of **11** was achieved by selectively converting the α-carboxylic acid into a mixed anhydride using isobutylchloroformate and triethylamine.[25] Isoglutamine **13** was obtained as a hydrochloric acid salt by hydrogenolysis of the carboxybenzyl (Cbz) protecting group of **12** and subsequent recrystallization with concentrated hydrochloric acid. Isoglutamine benzyl ester **15** was generated in good yield through benzylation of amide **14**, which was produced by protection of the isoglutamine hydrochloric acid salt **13** with Boc anhydride.[44] This optimized route enabled the preparation of multi-gram quantities (>20 grams) of **15** in four steps, requiring only one silica gel chromatography operation. Subsequent removal of the *tert*-butyloxycarbonyl (Boc) protecting group of **15** using TFA (13 equiv.) afforded **16**, [44] setting the stage for the peptide coupling between **16** and Boc-L-alanine. Optimization of coupling conditions[45-48] identified the combination of 1-ethyl-3-(3-dimethylaminopropyl)carbodiimide (EDCI), 1-hydroxy-7-

azabenzotriazole (HOAt), and 2,2,6,6-tetramethylpiperidine (TMP) in dichloromethane (CH_2Cl_2) as optimal. Final deprotection of **17** afforded the primary amine used for the coupling of **8** and protected *N*-acetyl glucosamine **7a** and **7b**.

Scheme 3. Synthesis of dipeptide **8**[a]

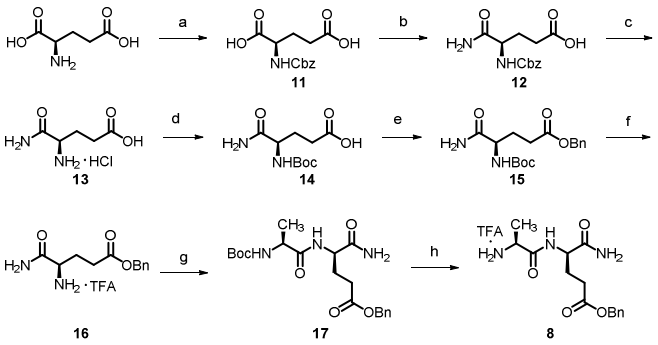

[a]Reagents and conditions: (a) CbzCl, $NaHCO_3/Na_2CO_3$, H_2O/Acetone, 0ºC to r.t., 36h, 92%; (b) 1. Isobutylchloroformate, NEt_3, THF, -30ºC, 30min; 2. NH_3 in THF solution, -30 ºC, 24h, 60%; (c) Pd/C (100 w/w%), H_2, AcOH/MeOH=1:1, r.t., 12h; (d) Boc_2O, Na_2CO_3, dioxane/H_2O, r.t., 12h; (e) BnBr, $NaHCO_3$, DMF, 60 ºC, 12h, 44% over four steps; (f) TFA, CH_2Cl_2, r.t., 4h; (g) Boc-L-alanine, EDCI, HOAt, TMP, CH_2Cl_2, r.t., 24h, 66% two steps; (h) TFA, CH_2Cl_2, r.t., 30min.

With **8**, **7a**, and **7b** in hand, our attention turned to the fragment coupling between **8** and carbohydrate **7a** and **7b** (Scheme 4). Gratifyingly, by employing the conditions of EDCI, HOAt, and TMP in CH_2Cl_2, **4** and **5** were formed cleanly after twelve hours. Analogs **6** and **3** were obtained by treating **4** and **5** with TFA in dichloromethane for one hour. [49]

Scheme 4. Fragment couplings to access MDP analogs[a]

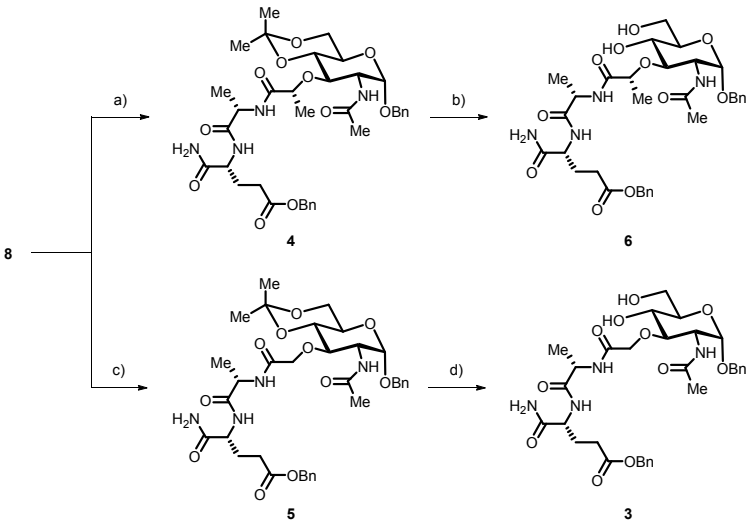

[a]Reagents and conditions: (a) **7a**, TMP ,EDCI, HOAt, CH_2Cl_2, r.t. 12h, 56%, two steps; (b) TFA, CH_2Cl_2, 0 °C, 1h, 73%; (c) **7b**, TMP ,EDCI, HOAt, CH_2Cl_2, r.t. 12h, 57%, two steps; (d) TFA, CH_2Cl_2, 0 °C, 1h, 63%.

2.5) Analysis of MDP analogs

MDP was shown earlier to express activity inhibiting the synthesis of TNF-α[7]. Therefore, we were interested in MDP-like compounds with improved anti-inflammatory potency (more typically nonspecific ester hydrolysis). Four MDP derivatives (**3**-**6**) were synthesized (Figure 8B) and further analyzed (Figures 9-11). As shown in Figures 9 and 10, among the four derivatives, only **4** was similar to MDP, in that it gradually reduced TNF-α as a result of an increased concentration and induced AP1/A20 gene expression. We also found that a high dose of analog **4** in macrophages reduced the transcription of RIP2, NOD2, and NFκB to an even greater extent than MDP treatment did (Figure 11). This indicates that, based on its efficacy, analog **4** is indeed an improved compound in comparison to MDP. To confirm our *in vitro* observations, *in vivo* *P.g*-induced endotoxic shock was performed[50]. As shown in Figure 12, *P.g*-injection-only induced septic shock, while death was precipitated with additional treatment of MDP-low.

However, injecting mice with MDP-high or analog **4** significantly reduced endotoxic shock and further prevented death.

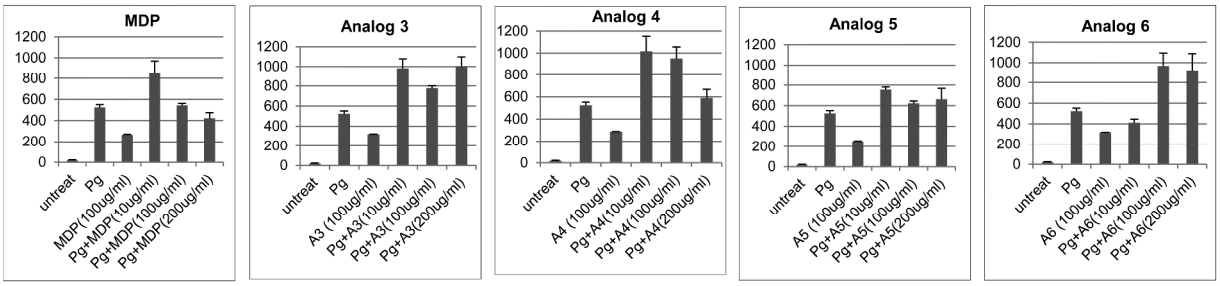

Figure 9. ELISA analysis of individual MDP or its derivative-mediated TNF-α gene expression. WT mouse macrophages were untreated or treated with *P.g* alone or the different MDP derivatives alone as the controls or co-treated with *P.g* plus 10, 100, 200 μg/ml of MDP or analogs **3-6** for 3 h. The media from each test group were used to detect TNF-α via an ELISA kit. Data are represented as Mean ±S.E. *≤0.05.

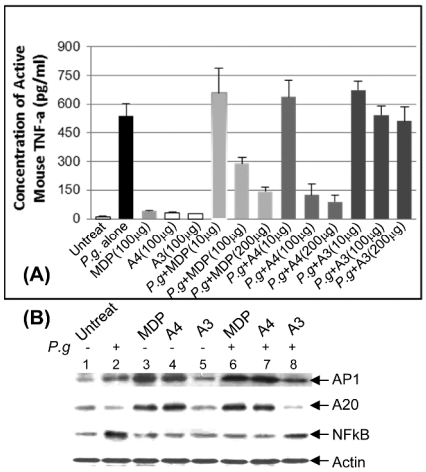

Figure 10. ELISA analysis of TNF-α production in response to *P.g* and/or MDP, analog **3**, or analog **4.** WT mouse macrophages were untreated or treated with *P.g*, MDP, analog **3**, or analog **4** as controls, or co-treated with *P.g* plus 10, 100, 200 μg/ml of MDP, analog **3**, or analog **4** for 3 h. The supernatants from each group were assessed by ELISA to detect the levels of TNF-α protein (**A**). The regulatory proteins from each group were detected by Western blot (**B**) using antibodies against AP1, A20, NFkB, or Actin as the control. Data were represented as Mean ± S.E. *p<0.05.

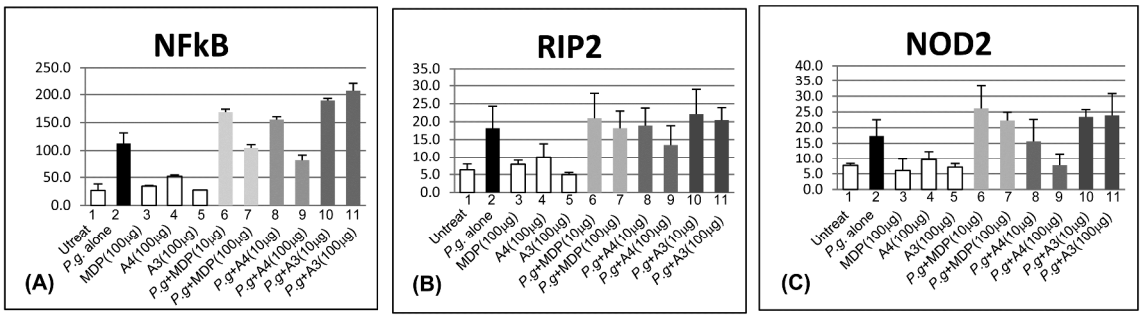

Figure 11. RT-PCR analysis of individual MDP or derivative-mediated gene expression. WT mouse macrophages were untreated or treated with *P.g* alone, or MDP, analog **3,** or analog **4** alone as the controls or co-treated with *P.g* plus 10, 100, 200 μg/ml of MDP, analog **3**, or analog **4** for 3 h. The total RNAs from each group were assessed by RT-PCR with the primers of NFkB (**A**), RIP2 (**B**), or NOD2 (**C**). GAPDH was used as a house keeping control gene for normalization. Data are represented as Mean ± S.E. *p<0.05.

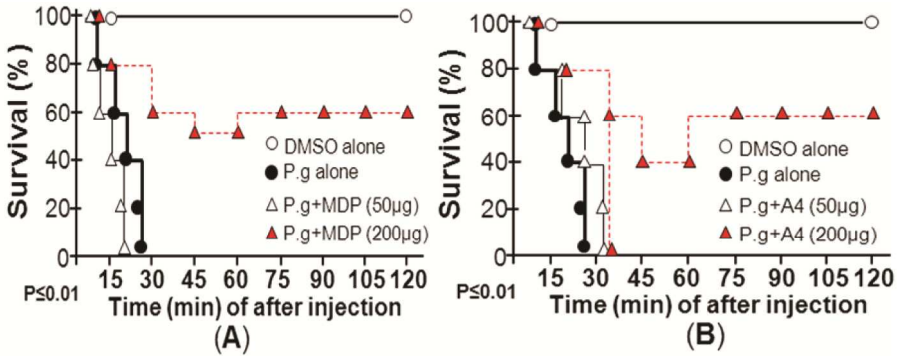

Figure 12. Analysis of endotoxic shock. WT mice were i.p. injected with 2 mg/kg (50 µg) of MDP-low (A) or the derivative analog **4** (B); 8 mg/kg (200 µg) of MDP-high (A) or analog **4** (B); or DMSO alone as the negative control. Following injection, they were immediately i.v. injected with *P.g* ($5x10^8$ cells/mouse). Mice were then monitored and their status was recorded. The *p*-value for the test groups (n=3) was calculated by the Wald's test in a discrete time hazard model using version 9.2 of SAS software gene for normalization. Data are represented as Mean ± S.E. *p<0.05.

3) CONCLUSIONS

Inflammatory and immune responses appear to be important mediators linking infection and systemic conditions, such as atherogenesis, possibly requiring residence of the pathogen in the vessel wall. Interestingly, the majority of pathogens associated with atherogenesis share four important characteristics: they are involved in common infections[51]; they are all intracellular pathogens[52]; they establish long-term persistent infections[53]; and they induce long-lasting increases in specific antibody production[54]. Specific cytosolic recognition molecules (e.g. NOD2) activated by MDP appear to be involved in this process, such that the infection itself is appropriate to drive the activation of signaling pathways.[55] We evaluated the role of NOD2 in two chronic inflammatory diseases: atherosclerosis and alveolar bone loss. *P.g*-challenged ApoE-/- mice injected with high doses of MDP displayed a reduction of serum cholesterol and inflammatory cytokines, alveolar bone loss, and atherosclerotic lesions, compared to the *P.g* challenged ApoE-/- mice injected with saline[7]. In the present study we present evidence

highlighting a high dose MDP-dependent signaling pathway which activates JNKs, induces AP1, up-regulates A20 expression, restricts NOD2, inhibits NFκB, and consequently, reduces *P.g*-induced TNF-α production in mouse macrophages. Furthermore, using the power of modern synthetic chemistry, we have described an efficient, highly convergent synthesis of enantiomerically enriched MDP analogs (**3-6)** by merging the suitably functionalized carbohydrate portion with the dipeptide fragment. The conformationally biased analog **4** was found to further improve MDP function and inhibition of *P.g*-induced pro-inflammatory activities. A novel signaling pathway leading to TNF-α expression that is influenced by exposing macrophages to both *P.g* and a high dose of MDP or analog **4** is hereto advocated. MDP-high and its optimized analog **4** both reduced *P.g*-induced septic shock and death—a clear indication of their potent anti-inflammatory effect. We propose that the rigid bicyclic ring system present on analog **4** is responsible for the enhanced reduction of TNF-α production and immunity to septic shock and death. The present work paves the way for further MDP optimization to improve its efficacy and safety.

4) EXPERIMENTAL SECTION

(A) Chemistry.

All reactions were carried out in oven or flame-dried glassware under argon atmosphere unless otherwise specified. Triethylamine and 2,2,6,6-tetramethylpiperidine were distilled over calcium hydride and stored over potassium hydroxide. Dichloromethane and tetrahydrofuran were obtained from a dry solvent system (alumina) and used without further drying. All other reagents were used as supplied. Unless otherwise noted, reactions were magnetically stirred and

monitored by thin layer chromatography with Macherey Nagel Polygram 0.20 mm silica gel 60 Å plates. Flash chromatography was performed on Sorbent Technologies 32-63 μm 60 Å silica gel. Yields refer to chromatographically and spectroscopically pure compounds, unless otherwise noted. ^{1}H and ^{13}C NMR spectra were taken in $CDCl_3$, DMSO-d6, and MeOH-d4 at 400 or 500 MHz (as indicated), respectively. Chemical shifts are reported in parts per million using the solvent internal standard (chloroform, 7.24 and 77.0 ppm, DMSO, 2.5 and 40.0 ppm, and MeOH, 3.31 and 49.0 ppm respectively). Data are reported as follows: chemical shift, multiplicity (s = singlet, d = doublet, t = triplet, q = quartet, m = multiplet, br = broad), coupling constant, integration. Infrared resonance spectra were recorded on a Nexus 670 FT-IR spectrometer. Optical rotations were recorded on a Rudolph Autopol II digital polarimeter at 589 nm and reported as follows: $[\alpha]_D^{20}$ (concentration in g/100 mL solvent and solvent). High resolution mass-spectra were obtained on a Waters Q-TOF Mass Spectrometer at the Boston University Chemical Instrumentation Center. The purity of all compounds were determined to be >95% by UPLC-MS.

***N*-((2*S*,3*R*,4*R*,5*S*,6*R*)-2-(benzyloxy)-4,5-dihydroxy-6-(hydroxymethyl)tetrahydro-2H-pyran-3-yl)acetamide (9):** *N*-acetyl-D-glucosamine (20 g, 9.04 mmol, 1.0 equiv) was suspended in 152 mL benzyl alcohol under argon at room temperature. Hydrogen chloride solution (4M in anhydrous 1,4-dioxane, 2.5 mL, 9.94 mmol, 1.1 equiv) was added drop-wise via a syringe. The mixture was heated at 95 ^{o}C for 4 h. After the reaction was complete, it was cooled down to room temperature, and then poured into 1L cold ether with vigorous stirring. The resulting brown cake was filtered, collected, and washed with cold ether. Purification by recrystallization from ethanol afforded **9** as a white solid as a single α-anomer (18g, 64% yield). $[\alpha]_D^{20}$= +153.2 (*c* 1.0, DMSO);

^{1}H NMR (500 MHz, DMSO-d6): δ7.80 (d, *J* = 8.5Hz, 1H), 7.36-7.25 (m, 5H), 5.00 (d, *J* = 6Hz, 1H), 4.71 (d, *J* = 6Hz, 1H), 4.68 (d, *J* = 3.5Hz, 1H, **anomeric**), 4.65 (d, *J* = 12.5Hz, 1H), 4.52 (t, *J* = 5.7Hz, 1H), 4.40 (d, *J* = 12.5 Hz, 1H), 3.68-3.62 (m, 2H), 3.53-3.42 (m, 3H), 3.16-3.11 (m, 1H), 1.81 (s, 3H);

^{13}C NMR (125 MHz, DMSO-d6): δ169.90, 138.37, 128.62, 127.95, 127.86, 96.33, 73.56, 71.34, 71.02, 68.13, 61.30, 54.20, 23.00;

IR (neat/cm^{-1}) υ_{max} : 3288, 2908, 1637, 1549, 1124, 1039

HRMS (ESI) *m/z* calcd for $C_8H_{15}NO_6$ $[M+H]^+$ 312.1447, found 312.1443;

UPLC T_R 0.72 min.

***N*-((4a*R*,6*S*,7*R*,8*R*,8a*S*)-6-(benzyloxy)-8-hydroxy-2,2-dimethylhexahydropyrano[3,2-d][1,3]dioxin-7-yl)acetamide (10): 9**(18 g, 57.8 mmol, 1 equiv) was suspended in 288 mL acetone under argon. 2,2-dimethoxypropane (72 mL,578.2 mmol, 10 equiv) was added in, followed by *p*-toluenesulfonic acid monohydrate (*p*-TSA·H_2O) (1.09g, 5.76 mmol, 0.1 equiv). The mixture was stirred at room temperature for 12 h. The reaction was quenched and neutralized with saturated sodium bicarbonate solution. The aqueous layer was extracted with dichloromethane (3 x 500 mL), and the combined organic layers were dried over $MgSO_4$, filtered, and concentrated to obtain pure **10** (20g, 100% yield). $[\alpha]_D^{20}$= +86.4 (*c* 1.0, CH_2Cl_2);

^{1}H NMR (500 MHz, $CDCl_3$): δ7.40-7.30 (m, 5H), 5.86 (d, *J* = 8.5Hz, 1H), 4.88 (d, *J* = 3.5Hz, 1H, **anomeric**), 4.71 (d, *J* = 12.0Hz, 1H), 4.45 (d, *J* = 12.0Hz, 1H), 4.17 (dt, *J* = 10.0, 4.0Hz, 1H), 3.84-3.60 (m, 5H), 1.98 (s, 3H), 1.52 (s, 3H), 1.43 (s, 3H);

^{13}C NMR (125 MHz, $CDCl_3$): δ171.41, 136.79, 128.65, 128.27, 128.07, 99.87, 97.16, 74.70, 70.95, 69.83, 63.66, 62.20, 54.08, 29.07, 23.25, 19.08;

IR (neat/cm^{-1}) υ_{max} : 3319, 1656, 1546, 1372, 1267, 1199, 1122, 1073;

HRMS (ESI) *m/z* calcd for $C_{18}H_{25}NO_6$ $[M+Na]^+$ 374.1580, found 374.1589;

UPLC T_R 1.09 min.

(*R*)-2-(((4a*R*,6*S*,7*R*,8*R*,8a*S*)-7-acetamido-6-(benzyloxy)-2,2-dimethylhexahydropyrano[3,2-d][1,3]dioxin-8-yl)oxy)propanoic acid (7a): Sodium hydride (1.5g, 60% dispersion in mineral oil, 37.5 mmol, 3 equiv) was washed with hexanes (3 mL) three time to remove mineral oil, and was suspended in 42 mL THF under argon. **10** (4.4g, 12.5 mmol, 1 equiv) was added into the above solution slowly, followed by (*S*)-2-chloropropanoic acid (1.3 mL, 15.0 mmol, 1.2 equiv) drop-wise. The resulting mixture was stirred vigorously at room temperature until there was no gas evolution. Then it was heated at 50 ^oC for 18 h (max speed of stirring). The reaction mixture was cooled down to room temperature, quenched with 40mL DI water, and acidified with phosphoric acid to pH=3. It was then extracted with dichloromethane (3 x 300 mL), and the combined organic layers were dried over $MgSO_4$, filtered, and concentrated. Purification over silica gel chromatography (50% EtOAc/CH_2Cl_2, then 4% MeOH/CH_2Cl_2) afforded product **7a** as a fluffy, white solid (4.5g, 85% yield). $[\alpha]_D^{20}$= +118.4 (*c* 1.0, CH_2Cl_2);

^{1}H NMR (500 MHz, $CDCl_3$): δ7.45 (d, *J* = 5.2Hz, 1H), 7.35-7.28 (m, 5H), 5.26 (d, *J* = 3.6Hz, 1H, **anomeric**), 4.65 (d, *J* = 11.9Hz, 1H), 4.47 (d, *J* = 11.9Hz, 1H), 4.40 (q, *J* = 7.1Hz, 1H), 3.94-3.90 (m, 1H), 3.82-3.65 (m, 5H), 2.00 (s, 3H), 1.51 (s, 3H), 1.42 (d, *J* = 7.1Hz, 3H), 1.40 (s, 3H);

^{13}C NMR (125 MHz, $CDCl_3$): δ177.07, 172.49, 137.21, 128.39, 127.89, 127.87, 99.57, 96.78, 75.77, 75.38, 75.24, 70.11, 63.77, 62.43, 54.56, 29.16, 22.60, 19.24, 18.73;

IR (neat/cm^{-1}) υ_{max} : 3298, 2992, 2942, 2880, 1716, 1621, 1565, 1455, 1383, 1267, 1237, 1202, 1175, 1149, 1123, 1076, 1046;

HRMS (ESI) *m/z* calcd for $C_{21}H_{29}NO_8$ $[M+Na]^+$ 446.1791, found 446.1794;

UPLC T_R 1.30 min.

2-(((4a*R*,6*S*,7*R*,8*R*,8a*S*)-7-acetamido-6-(benzyloxy)-2,2-dimethylhexahydropyrano[3,2-d][1,3]dioxin-8-yl)oxy)acetic acid (7b): Sodium hydride (2.19g, 60% dispersion in mineral oil, 45.6 mmol, 4 equiv) was washed with hexanes (4 mL) three time to remove mineral oil, and was suspended in 60 mL THF under argon. **10** (4.0 g, 11.4 mmol, 1 equiv) was added into the above solution slowly, followed by bromoacetic acid (2.225 g, 16.0 mmol, 1.4 equiv) dropwise. The resulting mixture was stirred vigorously at room temperature until no gas evolution. Then it was heated at 50°C for 18 h (max speed of stirring). The reaction mixture was cooled down to room temperature, quenched with 100mL DI water, and acidified with phosphoric acid to pH=3. It was then extracted with dichloromethane (3 x 300 mL), and the combined organic layers were dried over $MgSO_4$, filtered, and concentrated. Purification over silica gel chromatography (3.7% MeOH/CH_2Cl_2) afforded product **7b** as a fluffy, white solid (3.9 g, 84% yield). $[\alpha]_D^{20}$= + 93.2 (*c* 1.0, CH_2Cl_2);

^{1}H NMR (500 MHz, $CDCl_3$): δ7.36-7.28 (m, 5H), 7.24 (d, *J* = 6.3Hz, 1H), 5.16 (d, *J* = 3.8 Hz, 1H, **anomeric**), 4.67 (d, *J* = 11.9Hz, 1H), 4.47 (d, *J* = 11.9 Hz, 1H), 4.31 (ABq, *J* = 17.6Hz, 2H), 4.01 (ddd, *J* = 10.2, 6.6, 3.8 Hz, 1H), 3.82-3.65 (m, 5H), 2.00 (s, 3H), 1.51 (s, 3H), 1.41 (s, 3H);

^{13}C NMR (125 MHz, $CDCl_3$): δ174.26, 172.53, 137.18, 128.42, 127.91, 127.84, 99.68, 96.74, 76.06, 75.58, 70.04, 68.32, 63.72, 62.30, 54.39, 29.11, 22.57, 19.18;

IR (neat/cm^{-1}) υ_{max} : 3309, 2995, 2932, 2882, 1719, 1621, 1560, 1433, 1383, 1267, 1233, 1201, 1174, 1146, 1119, 1074, 1042;

HRMS (ESI) *m/z* calcd for $C_{21}H_{29}NO_8$ $[M+Na]^+$ 432.1634, found 432.1628;

UPLC T_R 1.19 min.

((Benzyloxy)carbonyl)-D-glutamic acid (11): Glutamic acid (10g, 68 mmol, 1 equiv) was dissolved in 100 mL DI water at 0 ^{o}C (without Argon protection). Sodium carbonate (21.6g, 204 mmol, 3 equiv) and sodium bicarbonate (5.8g, 68 mmol, 1 equiv) were added sequentially. 10mL acetone was added into the above mixture, followed by benzyl chloroformate (20 mL, 150 mmol, 2.2 equiv). The resulting mixture was stirred for 36 h, gradually warming to room temperature. It was quenched by acidifying to pH=3 with 20% hydrochloric acid and extracted with EtOAc (3 x 500 mL). The combined organic layers were dried over $MgSO_4$, filtered, and concentrated. Purification over silica gel chromatography (5% MeOH/CH_2Cl_2) afforded product **11** as a white solid (17.5g, 92% yield). $[\alpha]_D^{20}$= +7.2 (*c* 1.0, MeOH);

^{1}H NMR (500 MHz, DMSO-d6): δ12.37 (br, 2H), 7.37-7.28 (m, 5H), 5.02 (s, 2H), 3.98 (td, *J* = 11.5, 5.0Hz, 1H), 2.32-2.26 (m, 2H), 1.98-1.91 (m, 1H), 1.78-1.70 (m, 1H);

^{13}C NMR (100 MHz, DMSO-d6): δ174.19, 174.06, 156.62, 137.40, 128.79, 128.26, 128.15, 65.87, 53.48, 30.52, 26.52;

IR (neat/cm^{-1}) υ_{max} : 3466, 3332, 3199, 1723, 1666, 1644, 1541, 1410, 1267, 1172, 1051;

HRMS (ESI) *m/z* calcd for $C_{13}H_{15}NO_6$ $[M+Na]^+$ 304.0797, found 304.0789;

UPLC T_R 0.82 min.

(*R*)-5-amino-4-(((benzyloxy)carbonyl)amino)-5-oxopentanoic acid (12): 11 (15g, 53.3 mmol, 1 equiv) was dissolved in 100mL THF under argon at room temperature. Freshly distilled triethylamine (16.4mL, 117.3 mmol, 2.2 equiv) was added dropwise into the above solution, and stirred for 15 min before moved to a -30 ^{o}C chiller. At -30 ^{o}C, isobutylchloroformate (8 mL, 64 mmol, 1.0 equiv) was added in dropwise, forming a heterogeneous mixture. It was stirred at -30 ^{o}C for 1h. Ammonia (266mL, 0.5M in THF, 133 mmol, 2.5 equiv) was added in slowly through the inner surface of the reaction flask. The reaction mixture was stirred at -30 ^{o}C for 48 h before

it was quenched by 200 mL DI water. The mixture was acidified to pH=3 by phosphoric acid. The resulting mixture was partitioned between 500 mL water and 500 mL ethyl acetate. The aqueous layer was extracted with EtOAc (3 x 500 mL). The combined organic layers were dried over $MgSO_4$, filtered, and concentrated. The crude material was used without purification. Pure product **12** was obtained by preparative thin layer chromatography (TLC) purification in 10% MeOH/CH_2Cl_2 for characterization (60% yield). $[\alpha]_D^{20}$= +8.2 (*c* 1.0, MeOH);

^{1}H NMR (500 MHz, DMSO-d6): δ12.07 (br, 1H), 7.35-7.29 (m, 5H), 7.00 (s, 1H), 5.00 (s, 2H), 3.92 (td, *J* = 8.8, 5.2Hz, 1H), 2.23 (t, *J* = 15.7Hz, 2H), 1.91-1.84 (m, 1H), 1.74-1.67 (m, 1H);

^{13}C NMR (100 MHz, DMSO-d6): δ174.32, 173.87, 156.38, 137.47, 128.76, 128.21, 128.11, 65.85, 54.31, 30.72, 27.63;

IR (neat/cm^{-1}) υ_{max} : 3465, 3331, 3202, 1723, 1666, 1647, 1609, 1541, 1410, 1352, 1267, 1172, 1052;

HRMS (ESI) *m/z* calcd for $C_{13}H_{16}N_2O_5$ $[M+Na]^+$ 303.0957, found 303.0963;

UPLC T_R 0.82 min.

(*R*)-1-amino-4-carboxy-1-oxobutan-2-aminium chloride (13): 12 (12g, 42.8 mmol, 1 equiv) was dissolved in a mixture of 75 mL methanol and 75 mL acetic acid at room temperature. Pd/C (10 wt. % loading, 10g, 80 w%) was added in. The internal atmosphere was exchanged with hydrogen gas by bubbling through hydrogen gas for 5 min. The reaction was stirred under an atmosphere of hydrogen gas (1 atm, balloon) for 12h. The reaction mixture was then filtered through a pad of celite and washed with dry methanol. The solvents were removed *in vacuo*. The remaining acetic acid was azeotropically removed with ethyl acetate *in vacuo* (it is important to make sure that all of the acetic acid was removed). The crude oil was recrystallized by dissolving

it in methanol and adding concentrated hydrochloric acid to it. The mother liquor was recrystallized twice until no more solids formed. **13** was obtained as a fluffy, white solid (9g, 62% yield) after air dry.

(*R*)-5-amino-4-((*tert*-butoxycarbonyl)amino)-5-oxopentanoic acid (14): A solution of **13** (7.5g, 51.0 mmol, 1 equiv) in 44 mL DI water was cooled to 0 ^{o}C (without Argon protection). Sodium carbonate (10.9g, 102.8 mmol, 2 equiv) was slowly added in to the mixture. The resulting solution was stirred for 10 min until it was clear. 36 mL of 1,4-dioxane was added in, followed by Di-*tert*-butyl dicarbonate (Boc_2O) (13.4g, 61.4 mmol, 1.2 equiv). The mixture was stirred at room temperature for 12h. It was quenched by phosphoric acid and the pH was adjusted to 3. The mixture was partitioned between 500 mL ethyl acetate and 500 mL DI water. The aqueous layer was extracted with EtOAc (3 x 500 mL). The combined organic layers were dried over $MgSO_4$, filtered, and concentrated. The crude material was used without purification.

Benzyl (*R*)-5-amino-4-((*tert*-butoxycarbonyl)amino)-5-oxopentanoate (15): Crude **14** (12.6g, 51.2 mmol, 1 equiv) was dissolved in 200 mL dry dimethylformamide (DMF) under argon. Sodium bicarbonate (12.9g, 153.6 mmol, 3 equiv) was added in one portion, followed by benzyl bromide (12 mL, 102.4 mmol, 2 equiv). The mixture was heated at 60 ^{o}C for 18 h. The reaction mixture was cooled down to room temperature, and neutralized by phosphoric acid. The resulting mixture was partitioned between 800 mL ethyl acetate and 500 mL DI water. The aqueous layer was extracted with EtOAc (3 x 100 mL). The combined organic layers were washed with 5% LiCl solution (8 x 200 mL) to remove most DMF. Then the organic layer was dried over $MgSO_4$, filtered, and concentrated. Purification over silica gel chromatography (gradient, 3% to 4%, MeOH/CH_2Cl_2) afforded product **15** as a white solid (6.8g, 44% yield over two steps). $[\alpha]_D^{20}$= +4.6 (*c* 1.0, CH_2Cl_2);

^{1}H NMR (500 MHz, $CDCl_3$): δ7.39-7.30 (m, 5H), 6.30 (br, 1H), 5.65 (br, 1H), 5.33 (br, 1H), 5.13 (s, 2H), 4.21 (br, 1H), 2.57 (td, *J* = 16.9, 7.4Hz, 1H), 2.46 (td, *J* = 16.9, 7.0Hz, 1H), 2.20-2.13 (m, 1H), 1.97-1.90 (m, 1H), 1.43 (s, 9H);

^{13}C NMR (125 MHz, $CDCl_3$): δ174.45, 173.00, 155.82, 135.74, 128.53, 128.23, 128.17, 79.96, 66.46, 53.24, 30.40, 28.31, 27.89;

IR (neat/cm^{-1}) υ_{max} : 3384, 3348, 3184, 2978, 1727, 1682, 1519, 1450, 1391, 1366, 1278, 1250, 1165;

HRMS (ESI) *m/z* calcd for $C_{17}H_{24}N_2O_5$ $[M+Na]^+$ 359.1583, found 359.1582;

UPLC T_R 1.30 min.

(*R*)-1-amino-5-(benzyloxy)-1,5-dioxopentan-2-aminium 2,2,2-trifluoroacetate (16): A solution of **15** (500mg, 1.5 mmol, 1 equiv) in 13 mL dry CH_2Cl_2 under argon was added in TFA (1.5 mL, 19.6 mmol, 13 equiv) drop-wise. The resulting solution was stirred at room temperature for 4h. The solvent was removed *in vacuo*. The crude product **16** was used without purification.

Benzyl (*R*)-5-amino-4-((*S*)-2-((*tert*-butoxycarbonyl)amino)propanamido)-5-oxopentanoate (17): 16 (525mg, 1.5 mmol, 1 equiv) was taken up in dry dichloromethane and Boc-L-alanine (227mg, 1.2 mmol, 0.8 equiv) was added under argon. The resulting mixture was cooled down to 0 ^{o}C. TMP (1.3 mL, 7.5 mmol, 5 equiv) was added dropwise into the above mixture. It was stirred for 5 min before HOAt (306mg, 2.25 mmol, 1.5 equiv) and EDCI (349 mg, 2.25 mmol, 1.5 equiv) were added. The reaction mixture was stirred for 18 h, gradually warming to room temperature. The reaction was quenched by neutralizing it with saturated ammonia chloride solution. The mixture was partitioned between 100mL DI water and 100 mL dichloromethane. The aqueous layer was extracted with dichloromethane (3 x 100mL). The combined organic layers were dried over $MgSO_4$, filtered, and concentrated. Purification over silica gel

chromatography (4% MeOH/CH_2Cl_2) afforded product **17** (403mg, 66% over two steps) as a fluffy, white solid. $[\alpha]_D^{20}$= +1.4 (*c* 1.0, CH_2Cl_2);

^{1}H NMR (500 MHz, $CDCl_3$): δ7.38-7.30 (m, 5H), 7.26 (br, 1H), 6.80 (br, 1H), 5.75 (br, 1H), 5.19 (d, *J* =3.1, 1H), 5.12 (ABq, *J* = 12.3 Hz, 2H), 4.48 (dd, *J* = 10, 7.5Hz, 1H), 4.07, (dq, *J* = 7.1, 3.1Hz, 1H), 2.57 (dt, *J* = 16.9, 7.3Hz, 1H), 2.46 (dt, *J* = 17.0, 6.8 Hz, 1H), 2.26-2.19, (m, 1H), 2.05-1.98 (m, 1H), 1.41 (s, 9H), 1.32 (d, *J* = 7.1Hz, 3H);

^{13}C NMR (125 MHz, $CDCl_3$): δ173.50, 173.42, 173.32, 155.84, 135.62, 128.57, 128.32, 128.25, 80.38, 66.64, 52.27, 50.64, 30.58, 28.26, 26.77, 17.75;

IR (neat/cm^{-1}) υ_{max} : 3303, 2980, 2936, 1665, 1520, 1455, 1367, 1249, 1164, 1069, 1022;

HRMS (ESI) *m/z* calcd for $C_{20}H_{29}N_3O_6$ $[M+Na]^+$ 430.1954, found 430.1951;

UPLC T_R 1.25 min.

(*S*)-1-(((*R*)-1-amino-5-(benzyloxy)-1,5-dioxopentan-2-yl)amino)-1-oxopropan-2-aminium 2,2,2-trifluoroacetate (8): A solution of **17** (400mg, 0.98 mmol, 1 equiv) in 21 mL dry dichloromethane was added TFA (2.2 mL, 28.8 mmol, 29 equiv) dropwise under argon. The reaction mixture was stirred at room temperature for 1 h. The solvent was removed *in vacuo*. The remaining TFA was azeotropically removed with ethyl acetate *in vacuo*. The crude product **8** was used without purification.

Benzyl (*R*)-4-((*S*)-2-((*R*)-2-(((4a*R*,6*S*,7*R*,8*R*,8a*S*)-7-acetamido-6-(benzyloxy)-2,2-dimethylhexahydropyrano[3,2-d][1,3]dioxin-8-yl)oxy)propanamido)propanamido)-5-amino-5-oxopentanoate (4): A solution of **8** (249mg, 0.59 mmol, 1 equiv) in 6 mL dichloromethane was added **7a** (200mg, 0.47 mmol, 0.8 equiv) under argon at 0 ^oC. To the above solution, TMP (0.7 mL, 4.13 mmol, 7 equiv) was added dropwise. The resulting solution was stirred for 5 min. HOAt (120mg, 0.89 mmol, 1.5 equiv), followed by EDCI (138 mg, 0.89 mmol,

1.5 equiv) was added sequentially. The reaction mixture was stirred for 18 h, gradually warming to room temperature. The reaction was quenched by neutralizing it with saturated ammonia chloride solution. The mixture was partitioned between 100mL DI water and 100 mL dichloromethane. The aqueous layer was extracted with dichloromethane (3 x 100mL). The combined organic layers were dried over $MgSO_4$, filtered, and concentrated. Purification over silica gel chromatography (5% MeOH/CH_2Cl_2) afforded product **4** (188mg, 56% over two steps) as a fluffy, white solid. $[\alpha]_D^{20}$= +83.8 (*c* 1.0, CH_2Cl_2);

^{1}H NMR (500 MHz, $CDCl_3$): δ7.39-7.30 (m, 10H), 7.15 (d, *J* = 6.2Hz, 1H), 6.94 (s, 1H), 6.18 (d, *J* = 9.15Hz, 1H), 5.51 (s, 1H), 5.09 (s, 2H), 4.86 (d, *J* = 3.9Hz, 1H, **anomeric**), 4.68 (ABq, *J* = 11.9Hz, 1H), 4.48-4.44 (m, 1H), 4.45 (ABq, *J* = 11.8Hz), 4.23 (td, *J* = 9.6, 3.9Hz, 1H), 4.18-4.12 (m, 1H), 3.97 (q, *J* = 6.75Hz, 1H), 3.84-3.63 (m, 4H), 3.49 (dd, *J* = 9Hz, 1H), 2.57 (dt, *J* = 16.8, 7.3 Hz, 1H), 2.46 (dt, *J* = 17.2, 6.5 Hz, 1H), 2.24-2.18 (m, 1H), 2.07-2.00 (m, 1H), 1.92 (s, 3H), 1.50 (s, 3H), 1.40 (d, mix, 3H), 1.39, (s, 3H), 1.35 (d, *J* = 6.7, 3H);

^{13}C NMR (100 MHz, $CDCl_3$): δ174.36, 173.93, 173.31, 172.10, 170.61, 136.57, 135.47, 128.73, 128.62, 128.45, 128.35, 128.29, 128.06, 99.63, 97.35, 79.20, 78.39, 74.09, 69.96, 66.68, 63.90, 62.27, 52.82, 52.62, 49.94, 30.73, 29.09, 26.29, 23.52, 19.41, 19.04, 16.84;

IR (neat/cm^{-1}) υ_{max} : 3390, 3302, 3055, 2988, 2938, 1736, 1651, 1545, 1455, 1384, 1266, 1203, 1170, 1123, 1077, 1041;

HRMS (ESI) *m/z* calcd for $C_{36}H_{48}N_4O_{11}$ $[M+Na]^+$ 735.3217, found 735.3197;

UPLC T_R 1.44 min.

Benzyl (*R*)-4-((*S*)-2-(2-(((4a*R*,6*S*,7*R*,8*R*,8a*S*)-7-acetamido-6-(benzyloxy)-2,2-dimethylhexahydropyrano[3,2-d][1,3]dioxin-8-yl)oxy)acetamido)propanamido)-5-amino-5-oxopentanoate (5): A solution of **8** (249mg, 0.59 mmol, 1 equiv) in 6 mL dichloromethane was

added **7b** (192mg, 0.47 mmol, 0.8 equiv) under argon at 0 ^{o}C. To the above solution, TMP (0.7 mL, 4.13 mmol, 7 equiv) was added dropwise. The resulting solution was stirred for 5 min. HOAt (120mg, 0.89 mmol, 1.5 equiv), followed by EDCI (138 mg, 0.89 mmol, 1.5 equiv) was added sequentially. The reaction mixture was stirred for 18 h, gradually warming to room temperature. The reaction was quenched by neutralizing it with saturated ammonia chloride solution. The mixture was partitioned between 100mL DI water and 100 mL dichloromethane. The aqueous layer was extracted with dichloromethane (3 x 100mL). The combined organic layers were dried over $MgSO_4$, filtered, and concentrated. Purification over silica gel chromatography (5% MeOH/CH_2Cl_2) afforded product **5** (187mg, 56% over two steps) as a fluffy, white solid. $[\alpha]_D^{20}$= +59.8 (*c* 0.95, CH_2Cl_2);

^{1}H NMR (500 MHz, $CDCl_3$): δ7.39-7.29 (m, 10H), 6.93 (s, 1H), 6.12 (d, *J* = 9.3Hz, 1H), 5.66 (s, 1H), 5.10 (s, 2H), 4.84 (d, *J* =4.0Hz, 1H, **anomeric**), 4.70 (ABq, *J* =11.8Hz, 1H), 4.46 (ABq, *J* =11.8Hz, 1H), 4.45-4.41 (m, 1H), 4.34 (ABq, *J* =15.8Hz, 1H), 4.33-4.28 (m, 1H), 4.26 (dt, *J* = 9.7, 4Hz), 3.95 (ABq, *J* =15.7Hz, 1H), 3.84-3.66 (m, 4H), 3.51 (t, *J* = 9.2Hz, 1H), 2.53 (dt, *J* = 16.7, 7.3Hz, 1H), 2.43 (dt, *J* = 17.0, 6.8Hz, 1H), 1.93 (s, 3H), 1.49 (3, 3H), 1.39 (s, 3H), 1.37 (d, *J* = 7.1Hz, 3H);

^{13}C NMR (100 MHz, $CDCl_3$): δ173.58, 173.52, 172.46, 170.77, 170.70, 136.51, 135.59, 128.74, 128.59, 128.44, 128.32, 128.27, 128.18, 99.78, 97.25, 79.47, 74.22, 70.71, 69.98, 66.60, 63.56, 62.19, 52.60, 52.39, 49.24, 30.70, 29.15, 26.29, 23.54, 19.18, 17.32.

IR (neat/cm^{-1}) υ_{max} : 3307, 2943, 1737, 1660, 1533, 1456, 1377, 1267, 1202, 1173, 1128, 1076, 1046;

HRMS (ESI) *m/z* calcd for $C_{35}H_{46}N_4O_{11}$ $[M+Na]^+$ 721.3061, found 721.3080;

UPLC T_R 1.40 min.

Benzyl (*R*)-4-((*S*)-2-((*R*)-2-(((2*S*,3*R*,4*R*,5*S*,6*R*)-3-acetamido-2-(benzyloxy)-5-hydroxy-6-(hydroxymethyl)tetrahydro-2H-pyran-4-yl)oxy)propanamido)propanamido)-5-amino-5-oxopentanoate (6): A solution of **4**(100mg, 0.14 mmol, 1 equiv) in 6 mL dry dichloromethane was added 0.65 mL TFA under argon at 0°C. The reaction mixture was stirred at 0 ^{o}C for 1 h. The reaction was quenched by neutralizing it with saturated aqueous sodium bicarbonate. The mixture was partitioned between 50mL DI water and 50 mL ethyl acetate. The aqueous layer was extracted with ethyl acetate (3 x 50mL). The combined organic layers were dried over $MgSO_4$, filtered, and concentrated. Purification over silica gel chromatography (8% MeOH/CH_2Cl_2) afforded product **6** (69mg, 73%) as a white solid. $[\alpha]_D^{20}$= +46.4 (*c* 0.75, CH_2Cl_2);

^{1}H NMR (500 MHz, CD_3OD): δ7.38-7.25 (m, 10H), 5.11 (s, 2H), 4.87 (d, *J* = 3.6Hz, 1H, **anomeric**), 4.72 (ABq, *J* = 12.0Hz, 1H), 4.50 (ABq, *J* = 12.0Hz, 1H), 4.36 (dd, *J* = 9.5, 4.7Hz, 1H), 4.32 (q, *J* = 6.7Hz, 1H), 4.24 (q, *J* = 7.1Hz, 1H), 3.97 (dd, *J* = 10.6, 3.6Hz, 1H), 3.81 (dd, *J* = 11.8, 2.1Hz, 1H), 3.73-3.62 (m, 3H), 3.51-3.48 (m, 1H), 2.44 (t, *J* = 7.6Hz, 2H), 2.25-2.18 (m, 1H), 1.93-1.86 (m, 1H), 1.89 (s, 3H), 1.36 (d, *J* = 7.0Hz, 6H).

^{13}C NMR (100 MHz, CD_3OD): δ174.85, 174.73, 173.78, 172.68, 172.00, 137.38, 136.10, 128.11, 127.98, 127.80, 127.77, 127.48, 96.03, 79.40, 76.83, 72.74, 69.93, 68.77, 66.00, 61.12, 53.36, 52.15, 49.37, 29.96, 26.57, 21.41, 18.20, 16.35;

IR (neat/cm^{-1}) υ_{max} : 3373, 2933, 1655, 1545, 1456, 1204, 1136, 1026.

HRMS (ESI) *m/z* calcd for $C_{32}H_{42}N_4O_{11}$ $[M+Na]^+$ 681.2748, found 681.2764;

UPLC T_R 1.11 min.

Benzyl (*R*)-4-((*S*)-2-(2-(((2*S*,3*R*,4*R*,5*S*,6*R*)-3-acetamido-2-(benzyloxy)-5-hydroxy-6-(hydroxymethyl)tetrahydro-2H-pyran-4-yl)oxy)acetamido)propanamido)-5-amino-5-oxopentanoate (3): A solution of **5** (98mg, 0.14 mmol, 1 equiv) in 6 mL dry dichloromethane

was added 0.65 mL TFA under argon at 0°C. The reaction mixture was stirred at 0 °C for 1 h. The reaction was quenched by neutralizing it with saturated aqueous sodium bicarbonate. The mixture was partitioned between 50 mL DI water and 50 mL ethyl acetate. The aqueous layer was extracted with ethyl acetate (3 x 50 mL). The combined organic layers were dried over $MgSO_4$, filtered, and concentrated. Purification over silica gel chromatography (8% MeOH/CH_2Cl_2) afforded product **3** (58mg, 63%) as a white solid. $[\alpha]_D^{20}$= +62.2 (*c* 0.55, MeOH);

^{1}H NMR (500 MHz, CD_3OD): δ7.40-7.27 (m, 10H), 5.11 (s, 2H), 4.83 (d, *J* = 3.7Hz, 1H, **anomeric**), 4.74 (ABq, *J* = 11.9Hz, 1H), 4.51 (ABq, *J* = 11.9Hz, 1H), 4.37 (dd, *J* = 9.6, 4.7Hz, 1H), 4.32 (q, *J* = 7.1Hz, 1H), 4.21 (ABq, *J* = 16.1Hz, 2H), 4.05 (dd, *J* = 10.3, 3.6Hz, 1H), 3.82 (d, *J* = 9.9Hz, 1H), 3.74-3.57 (m, 4H), 2.45 (t, *J* = 7.5Hz, 2H), 2.26-2.19 (m, 1H), 1.94 (s, 3H), 1.94-1.87 (m, 1H), 1.37 (d, *J* = 7.2Hz, 3H);

^{13}C NMR (100 MHz, CD_3OD): δ174.73, 173.85, 172.74, 172.04, 172.00, 137.35, 136.10, 128.11, 128.04, 128.00, 127.79, 127.77, 127.53, 96.22, 81.70, 72.76, 70.92, 70.12, 68.88, 66.03, 60.98, 53.18, 52.21, 49.12, 30.03, 26.51, 21.26, 16.31;

IR (neat/cm^{-1}) υ_{max} : 3306, 2925, 1733, 1654, 1543, 1455, 1385, 1333, 1259, 1158, 1126, 1039;

HRMS (ESI) *m/z* calcd for $C_{33}H_{44}N_4O_{11}$ $[M+H]^+$ 673.3085, found 673.4091;

UPLC T_R 1.11 min.

(B) Biological Methods and Materials.

Animals and cells

8 to 10 week-old WT (C57BL/6) mice from The Jackson Laboratory were maintained under strict specific pathogen-free conditions. RAW264.7 cells (TIB 71, ATCC) and mouse primary peritoneal macrophages were cultured in a RPMI 1640 media (Cat#: 11875-093, Life

Technologies, NY) with 10% FBS at 37ºC in a 5% CO_2 atmosphere. Cells were treated with LPS, MDP or others as described below.

All mice protocols used in this study were approved by the Boston University Animal Care and Use Committee. All mice were obtained and used in compliance with institutional regulations and related federal, state, and local laws.

DNA constructs

A full-length mouse AP1 cDNA (Locus: AK135023, aa 1~335, Open Biosystems) was used as a template; the primer pairs 5'-atgactgcaaagatggaaac-3' and 5'-tcaaaacgtttgcaactgct-3' were used to amplify the full-length AP1 cDNA fragments by PCR. The DNA fragment was then sub-cloned into pcDNA3HA[56] (named AP1). The mouse genomic DNA (isolated by our lab) served as a template DNA, and primer pairs (5'- cagggaaagatgtccatatg-3' & 5'-gtcctcgacaaggcctgaag-3') were used to amplify A20 promoter DNA fragments (-1051~ -1 of A20, Locus: JN960089) by PCR. The DNA fragments were then sub-cloned into a pGL3-basic vector (Promega).

Luciferase assay

A commercial kit was used (Cat# E1500, Promega) and the assay was performed according to the protocols provided by the manufacturer.

Real-time PCR

The total mRNA purified from each test group was subjected to RT-PCR using RT-PCR kits (iScript & iQ SYBR Green, Bio-Rad) and the following primers: NOD2 (5'- gtgacatgtgctcacagg-3' & 5'-agcagccagtctaagatgct-3'), RIP2 (5'-atgaacggggacgccatctg-3'& 5'-acgagaccgtgccagaggcg-3'), A20 (5'-gctgaacaacttcttcctca-3'& 5'-atcccattggtaggtttgaa-3'), or NFkB (5'-atggcagacgatgatcccta-3'& 5'-gtatttctggtgaatataat-3'). The PCR products were then normalized to GAPDH mRNA levels following the manufacturer's protocols.

***In vivo* assay for LPS and/or MDP**

The 8 to 10 week-old WT mice were i.p. injected with DMSO alone as the negative control, *P.g* alone ($1x10^8$/kg) as the positive control, or co-treated with *P.g* ($1x10^8$/kg) and 2 mg/kg (50μg) of MDP-low or 8 mg/kg (200μg) of MDP-high (50ug or 200ug/mouse) among the test group subjects. All animals were continuously monitored for endotoxic response for 2 h after injection (n = 3 per group). The data were analyzed and then graphed (see Figure 12).

ELISA

Using an Invitrogen kit (Cat#: KMC30110), the conditioned media from mouse primary peritoneal macrophages were subjected to ELISA for the detection of TNF-α concentration, following the manufacturer's instructions. The ELISA-indicated immunoreactivities were quantified by using a microplate reader (Model 680, Bio-Rad). Data were analyzed and then graphed.

Chromatin immunoprecipitation (ChIP)

The assay was performed using a commercial kit (Cat#: 53009, ChIP-IT Express Enzymatic, Active Motif), with some modifications. RAW264.7 cells were treated with MDP-high or MDP-low concentrations for 3 hrs or transfected with 1 μg of the AP1 DNA overnight. 10 μg nuclear extracts as described,[57] as input from the cross-linked cells, were immunoprecipitated (IP) with 1 μg of the AP1 antibody or 1 μg of normal mouse IgG as the control at 4ºC for 4 hrs. DNA from each experimental group (Input or immunoprecipitated) was isolated by elution, reverse cross-linking and proteinase K treatment, according to the kit manufacturer's instructions. The DNA was then used as a template to perform PCR with A20 primers (5'-aaactatttgctgccttgta-3'& 5'-cactgaagaccaccaccatt-3') for amplification of a 100 bp DNA fragment of the A20 promoter or GAPDH primers (Invitrogen) as the control.

Western blotting

Cells were harvested and proteins from the whole cell and from the nuclei were fractionally purified. Nuclear proteins were purified by scraping treated and untreated cells. Pellets were held on ice for 15 min and in the presence of 25 μL 1% Nonidet P-40. They were re-suspended in 400 μL of cold buffer A (10 mM Hepes, pH 7.9/10 mM, KCl/0.1 mM, EDTA/0.1 mM, EGTA/1 mM, DTT/0.5 mM, phenylmethylsulfonyl fluoride/1 μg/ml, pepstatin A/10 μg/ml, leupeptin/10 μg/ml, aprotinin). Samples were vortexed and centrifuged for 1 min at 10,000 × g, and the pellets were again suspended with 100 μL of buffer B (20 mM Hepes, pH 7.9/400 mM, NaCl/1 mM, EDTA/1 mM, EGTA/1 mM, DTT/0.5 mM, phenylmethylsulfonyl fluoride/1 μg/ml, pepstatin A/10 μg/ml, leupeptin/10 μg/ml, aprotinin). After shaking the samples on a rocker platform for 15 min at 4°C, they were centrifuged at 4°C for another 15 min at 10,000 × g. Cell lysates from whole cells or nuclei (60 μg total proteins per lane) were applied to SDS polyacrylamide gels, and the proteins were detected by Western blot using antibodies directed against AP1 (sc-14027), A20 (sc-22834), NF□B (sc-372), p21 (sc-6246), p53 (sc-17846), NOD2 (sc-30199), MyD88 (sc-8196), GAPDH (sc-365062), or actin (sc-1615) (Santa Cruz Biotechnology). The Ub antibody (sc-271289, Santa Cruz Biotechnology) was used for detection of mouse ubiquitin and polyubiquitin.

Trypan blue exclusion method

To determine cell survival rates after toxicity tests, the Trypan blue exclusion method (Triangle Research Laboratories) was used. (Link: http:// triangleresearchlabs.net/wp-content/uploads/2012/06/Trypan-Blue-Cell-Counting-Protocol.pdf).

MDP

MDP was purchase from INVIVOGEN (tlrl-mdp, San Diego, CA) and was diluted to either a high concentration (100 μg/ml) or a low concentration (10 μg/ml).

Statistical analysis

All experiments were performed in triplicate and statistical analyses were conducted with the SAS software package. All data were normally distributed. For multiple mean comparisons, we conducted analysis of variance (ANOVA) tests, while using the Student's t-test for single mean comparisons. For time-course studies, we used a two-way repeated measure ANOVA. *P*-values less than 0.05 were considered significant.

5) SUPPORTING INFORMATION

Supporting information: ^{1}H and ^{13}C NMR spectra and structural confirmation of **9** and **12** and UPLC data for all compounds.

6) AUTHOR INFORMATION

***Corresponding Authors**

Phone: 617-638-4983. E-mail: samar@bu.edu

Center for Anti-Inflammatory Therapeutics, 650 Albany St., Rm. 343, Boston, MA 02118

Phone: 617-353-2484. E-mail: panek@bu.edu

Department of Chemistry, 24 Cummington St, Rm. 905, Boston, MA 02215

Notes

The authors declare no competing financial interest.

7) FUNDING

This work was supported by a grant from the NHLBI (RO1HL076801).

8) ACKNOWLEDGEMENTS

We are grateful to Mr. Chirag Patel (Department of Chemistry, Boston University), Mr. Shiheng Fan (Department of Chemistry, Boston University), Mr. Matthew Castello (Department of Chemistry, Boston University), Mr. Christopher Breen (Department of Chemistry, Boston University) for preparation of starting materials, preliminary results, Dr. Paul Ralifo and Dr. Norman Lee at the Boston University Chemical Instrumentation Center for helpful discussions and assistance with NMR and HRMS.

8) ABBREVIATIONS USED

Pattern recognition receptors (PRRs), Toll-like receptors (TLRs), nucleotide-binding oligomerization domain (NOD), NOD-like receptors (NLRs), caspase recruitment domains (CARDs), central NOD (NACHT) domain, Leu-rich repeats (LRRs), muramyl dipeptide (MDP), receptor-interacting protein 2 (RIP2), inhibitor of κB (IκB), mitogen-activated protein (MAP), interleukin-6 (IL-6), 10 μg/ml of MDP (MDP-low), 100 μg/ml or higher of MDP (MPD-high), ubiquitin-editing enzyme (A20), *Porphyromonas gingivalis (P.g),* activator protein 1 (AP1), Jun *N*-terminal kinases (JNKs), aminosaccharide compound (DFK1012), tetrahydrofuran (THF), Heteronuclear Single Quantum Coherence (HSQC), Heteronuclear Multiple Bond Correlation (HMBC), *p*-toluenesulfonic acid monohydrate (*p*-TsOH), trifluoroacetic acid (TFA), carboxybenzyl (Cbz), *tert*-butyloxycarbonyl (Boc), 1-ethyl-3-(3-dimethylaminopropyl)carbodiimide (EDCI), 1-hydroxy-7-azabenzotriazole (HOAt), 2,2,6,6-

tetramethylpiperidine (TMP), dichloromethane (CH_2Cl_2), thin layer chromatography (TLC), dimethylformamide (DMF), immunoprecipitation (IP), analysis of variance (ANOVA).

9) REFERENCES

(1) Mogensen, T. H. Pathogen recognition and inflammatory signaling in innate immune defenses. *Clin. Microbiol. Rev.* **2009**, *22*, 240-273.

(2) Maharana, J.; Dehury, B.; Sahoo, J. R.; Jena, I.; Bej, A.; Panda, D.; Sahoo, B. R.; Patra, M. C.; Pradhan, S. K. Structural and functional insights into CARDs of zebrafish (Danio rerio) NOD1 and NOD2, and their interaction with adaptor protein RIP2. *Mol. Biosyst.* **2015**, *11*, 2324-2336.

(3) Ver Heul, A. M.; Fowler, C. A.; Ramaswamy, S.; Piper, R. C. Ubiquitin regulates caspase recruitment domain-mediated signaling by nucleotide-binding oligomerization domain-containing proteins NOD1 and NOD2. *J. Biol. Chem.* **2013**, *288*, 6890-6902.

(4) Maharana, J.; Sahoo, B. R.; Bej, A.; Jena, I.; Parida, A.; Sahoo, J. R.; Dehury, B.; Patra, M. C.; Martha, S. R.; Balabantray, S.; Pradhan, S. K.; Behera, B. K. Structural models of zebrafish (Danio rerio) NOD1 and NOD2 NACHT domains suggest differential ATP binding orientations: insights from computational modeling, docking and molecular dynamics simulations. *PloS one* **2015**, *10*, e0121415.

(5) Strober, W.; Murray, P. J.; Kitani, A.; Watanabe, T. Signaling pathways and molecular interactions of NOD1 and NOD2. *Nat. Rev. Immunol.* **2006**, *6*, 9-20.

(6) Hedl, M.; Li, J.; Cho, J. H.; Abraham, C. Chronic stimulation of Nod2 mediates tolerance to bacterial products. *Proc. Natl. Acad. Sci. USA* **2007**, *104*, 19440-19445.

(7) Yuan, H.; Zelka, S.; Burkatovskaya, M.; Gupte, R.; Leeman, S. E.; Amar, S. Pivotal role of NOD2 in inflammatory processes affecting atherosclerosis and periodontal bone loss. *Proc. Natl. Acad. Sci. USA* **2013**, *110*, E5059-5068.

(8) Pauleau, A. L.; Murray, P. J. Role of nod2 in the response of macrophages to toll-like receptor agonists. *Mol. Cell. Biol.* **2003**, *23*, 7531-7539.

(9) Bertin, J.; Nir, W. J.; Fischer, C. M.; Tayber, O. V.; Errada, P. R.; Grant, J. R.; Keilty, J. J.; Gosselin, M. L.; Robison, K. E.; Wong, G. H.; Glucksmann, M. A.; DiStefano, P. S. Human CARD4 protein is a novel CED-4/Apaf-1 cell death family member that activates NF-kappaB. *J. Biol. Chem.* **1999**, *274*, 12955-12958.

(10) Iwanaga, Y.; Davey, M. P.; Martin, T. M.; Planck, S. R.; DePriest, M. L.; Baugh, M. M.; Suing, C. M.; Rosenbaum, J. T. Cloning, sequencing and expression analysis of the mouse NOD2/CARD15 gene. *Inflamm. Res.* **2003**, *52*, 272-276.

(11) Bertrand, M. J.; Doiron, K.; Labbe, K.; Korneluk, R. G.; Barker, P. A.; Saleh, M. Cellular inhibitors of apoptosis cIAP1 and cIAP2 are required for innate immunity signaling by the pattern recognition receptors NOD1 and NOD2. *Immunity* **2009**, *30*, 789.

(12) Claes, A.-K.; Steck, N.; Schultz, D.; Zähringer, U.; Lipinski, S.; Rosenstiel, P.; Geddes, K.; Philpott, D. J.; Heine, H.; Grassl, G. A. Salmonella enterica serovar typhimurium ΔmsbB triggers exacerbated inflammation in Nod2 deficient mice. *PloS one* **2014**, *9*, e113645.

(13) Hedl, M.; Abraham, C. Distinct roles for Nod2 protein and autocrine interleukin-1beta in muramyl dipeptide-induced mitogen-activated protein kinase activation and cytokine secretion in human macrophages. *J. Biol. Chem.* **2011**, *286*, 26440-26449.

(14) Lee, K. H.; Biswas, A.; Liu, Y. J.; Kobayashi, K. S. Proteasomal degradation of Nod2 protein mediates tolerance to bacterial cell wall components. *J. Biol. Chem.* **2012**, *287*, 39800-39811.

(15) Borm, M. E.; van Bodegraven, A. A.; Mulder, C. J.; Kraal, G.; Bouma, G. The effect of NOD2 activation on TLR2-mediated cytokine responses is dependent on activation dose and NOD2 genotype. *Genes Immun.* **2008**, *9*, 274-278.

(16) Huang, S.; Zhao, L.; Kim, K.; Lee, D. S.; Hwang, D. H. Inhibition of Nod2 signaling and target gene expression by curcumin. *Mol. Pharmacol.* **2008**, *74*, 274-281.

(17) Dzierzbicka, K.; Wardowska, A.; Trzonkowski, P. Recent developments in the synthesis and biological activity of muramylpeptides. *Curr. Med. Chem.* **2011**, *18*, 2438-2451.

(18) Kubasch, N.; Schmidt, R. R. Synthesis of muramyl peptides containing meso-diaminopimelic Acid. *Eur. J. Org. Chem.* **2002**, 2710.

(19) Kobayashi, S.; Fukuda, T.; Yukimasa, H.; Fujino, M.; Azuma, I.; Yamamura, Y. Synthesis of muramyl dipeptide analogs with enhanced adjuvant activity. *Bull. Chem. Soc. Jpn.* **1980**, *53*, 2570-2577.

(20) Wang, Z. F.; Xu, J. C. Synthesis of fluoro-containing muramyl dipeptide analogs. *Tetrahedron* **1998**, *54*, 12597-12608.

(21) Xing, S.; Gleason, J. L. A robust synthesis of *N*-glycolyl muramyl dipeptide via azidonitration/reduction. *Org. Biomol. Chem.* **2015**, *13*, 1515-1520.

(22) Hecker, S. J.; Minich, M. L. Synthesis of C(6)-carboxylate analogs of *N*-acetylmuramic acid. *J. Org. Chem.* **1990**, *55*, 6051-6054.

(23) Hiebert, C. K.; Kopp, W. C.; Richerson, H. B.; Barfknecht, C. F. Synthesis of a biologically-active fluorescent muramyl dipeptide congener. *J. Med. Chem.* **1983**, *26*, 1729-1732.

(24) Kiso, M.; Kaneda, Y.; Okumura, H.; Hasegawa, A.; Azuma, I.; Yamamura, Y. Synthesis and immunoadjuvant activities of muramoyl-L-alanyl-D-isoglutamine and some carbohydrate analogs. *Carbohydr. Res.* **1980**, *79*, C17-19.

(25) Charlotte, R. Convenient syntheses of L-Isoglutamine and L-Isoasparagine through derivatives commonly useful for peptide synthesis. *J. Am. Chem. Soc.* **1960**, *82*, 1641-1644.

(26) Melnyk, J. E.; Mohanan, V.; Schaefer, A. K.; Hou, C. W.; Grimes, C. L. Peptidoglycan modifications tune the stability and function of the innate immune receptor Nod2. *J. Am. Chem. Soc.* **2015**, *137*, 6987-6990.

(27) Shrikhande, G. V.; Scali, S. T.; da Silva, C. G.; Damrauer, S. M.; Csizmadia, E.; Putheti, P.; Matthey, M.; Arjoon, R.; Patel, R.; Siracuse, J. J.; Maccariello, E. R.; Andersen, N. D.; Monahan, T.; Peterson, C.; Essayagh, S.; Studer, P.; Padilha Guedes, R.; Kocher, O.; Usheva, A.; Veves, A.; Kaczmarek, E.; Ferran, C. O-Glycosylation regulates ubiquitination and degradation of the anti-Inflammatory protein A20 to accelerate atherosclerosis in diabetic apoE-null mice. *PloS one* **2010**, *5*, e14240.

(28) Da Silva, C. G.; Cervantes, J. R.; Studer, P.; Ferran, C. A20--an omnipotent protein in the liver: prometheus myth resolved? *Adv. Exp. Med. Biol.* **2014**, *809*, 117-139.

(29) Su, C.; Lichtenstein, G. R. Are there predictors of remicade treatment success or failure? *Adv. Drug Deliv. Rev.* **2005**, *57*, 237-245.

(30) Hitotsumatsu, O.; Ahmad, R. C.; Tavares, R.; Wang, M.; Philpott, D.; Turer, E. E.; Lee, B. L.; Shiffin, N.; Advincula, R.; Malynn, B. A.; Werts, C.; Ma, A. The ubiquitin-editing enzyme A20 restricts nucleotide-binding oligomerization domain containing 2-triggered signals. *Immunity* **2008**, *28*, 381-390.

(31) Shembade, N.; Ma, A.; Harhaj, E. W. Inhibition of NF-kappaB signaling by A20 through disruption of ubiquitin enzyme complexes. *Science (New York, N.Y.)* **2010**, *327*, 1135-1139.

(32) Kobayashi, K.; Inohara, N.; Hernandez, L. D.; Galan, J. E.; Nunez, G.; Janeway, C. A.; Medzhitov, R.; Flavell, R. A. RICK/Rip2/CARDIAK mediates signaling for receptors of the innate and adaptive immune systems. *Nature* **2002**, *416*, 194-199.

(33) Kobayashi, K. S.; Chamaillard, M.; Ogura, Y.; Henegariu, O.; Inohara, N.; Nunez, G.; Flavell, R. A. Nod2-dependent regulation of innate and adaptive immunity in the intestinal tract. *Science (New York, N.Y.)* **2005**, *307*, 731-734.

(34) Girardin, S. E.; Boneca, I. G.; Carneiro, L. A. M.; Antignac, A.; Jehanno, M.; Viala, J.; Tedin, K.; Taha, M. K.; Labigne, A.; Zahringer, U.; Coyle, A. J.; Bertin, J.; Sansonetti, P. J.; Philpott, D. J. Nod1 detects a unique muropeptide from Gram-negative bacterial peptidoglycan. *Science (New York, N.Y.)* **2003**, *300*, 1584-1587.

(35) Ellouz, F.; Adam, A.; Ciorbaru, R.; Lederer, E. Minimal structural requirements for adjuvant activity of bacterial peptidoglycan derivatives. *Biochem. Bioph. Res. Co.* **1974**, *59*, 1317-1325.

(36) Rubino, S. J.; Magalhaes, J. G.; Philpott, D.; Bahr, G. M.; Blanot, D.; Girardin, S. E. Identification of a synthetic muramyl peptide derivative with enhanced Nod2 stimulatory capacity. *Innate Immun.* **2013**, *19*, 493-503.

(37) Chamaillard, M.; Hashimoto, M.; Horie, Y.; Masumoto, J.; Qiu, S.; Saab, L.; Ogura, Y.; Kawasaki, A.; Fukase, K.; Kusumoto, S.; Valvano, M. A.; Foster, S. J.; Mak, T. W.; Nunez, G.; Inohara, N. An essential role for NOD1 in host recognition of bacterial peptidoglycan containing diaminopimelic acid. *Nat. Immunol.* **2003**, *4*, 702-707.

(38) Lee, K. H.; Liu, Y. J.; Biswas, A.; Ogawa, C.; Kobayashi, K. S. A novel aminosaccharide compound blocks immune responses by toll-like receptors and nucleotide-binding domain, leucine-rich repeat proteins. *J. Biol. Chem.* **2011**, *286*, 5727-5735.

(39) Hasegawa, A.; Okumura, H.; Nishibori, K.; Kaneda, Y.; Kiso, M.; Azuma, I. Studies on immunoadjuvant active compounds .14. The chemical modification of the C-2 substituent in the sugar moiety of *N*-acetylmuramoyl-L-Alanyl-D-isoglutamine, and the immunoadjuvant activities. *Carbohydr. Res.* **1981**, *97*, 337-345.

(40) Okumura, H.; Tokushima, Y.; Saiki, I.; Azuma, I.; Kiso, M.; Hasegawa, A. Studies on immunoadjuvant active compounds .22. Chemical modification of the C-6 substituent in the carbohydrate moiety of *N*-acetylmuramoyl-L-alanyl-D-isoglutamine (mdp), and the immunoadjuvant activity. *Carbohydr. Res.* **1983**, *122*, 87-98.

(41) Babic, A.; Pecar, S. Total synthesis of uridine diphosphate-*N*-acetylmuramoyl-L-alanine. *Tetrahedron Asymmetry* **2008**, *19*, 2265-2271.

(42) (a) It was discovered that the commercially available *N*-acetyl-D-glucosamine was contaminated with unidentifiable impurities which could not be easily removed. (b) The byproducts generated during benzyl protection were also found to have almost identical R_f values with compound **10**. We attributed this preference for the complete formation of the α-anomer to the thermodynamic reaction conditions.

(43) Pehere, A. D.; Abell, A. D. An improved large scale procedure for the preparation of *N*-Cbz amino acids. *Tetrahedron Lett.* **2011**, *52*, 1493-1494.

(44) Incerti, M.; Tognolini, M.; Russo, S.; Pala, D.; Giorgio, C.; Hassan-Mohamed, I.; Noberini, R.; Pasquale, E. B.; Vicini, P.; Piersanti, S.; Rivara, S.; Barocelli, E.; Mor, M.; Lodola, A. Amino acid conjugates of lithocholic acid as antagonists of the EphA2 Receptor. *J. Med. Chem.* **2013**, *56*, 2936-2947.

(45) Montalbetti, C. A. G. N.; Falque, V. Amide bond formation and peptide coupling. *Tetrahedron* **2005**, *61*, 10827-10852.

(46) Valeur, E.; Bradley, M. Amide bond formation: beyond the myth of coupling reagents. *Chem. Soc. Rev.* **2009**, *38*, 606-631.

(47) Han, Y. X.; Albericio, F.; Barany, G. Occurrence and minimization of cysteine racemization during stepwise solid-phase peptide synthesis. *J. Org. Chem.* **1997**, *62*, 4307-4312.

(48) Wilson, Z. E.; Fenner, S.; Ley, S. V. Total syntheses of linear polythiazole/oxazole Plantazolicin A and its biosynthetic precursor Plantazolicin B. *Angew. Chem. Int. Ed.* **2015**, *54*, 1284-1288.

(49) Hanessian, S.; Vakiti, R. R.; Dorich, S.; Banerjee, S.; Lecomte, F.; DelValle, J. R.; Zhang, J. B.; Deschenes-Simard, B. Total synthesis of Pactamycin. *Angew. Chem. Int. Ed.* **2011**, *50*, 3497-3500.

(50) Tang, X.; Metzger, D.; Leeman, S.; Amar, S. LPS-induced TNF-alpha factor (LITAF)-deficient mice express reduced LPS-induced cytokine: Evidence for LITAF-dependent LPS signaling pathways. *Proc. Natl. Acad. Sci. USA* **2006**, *103*, 13777-13782.

(51) Burgner, D. P.; Sabin, M. A.; Magnussen, C. G.; Cheung, M.; Sun, C.; Kahonen, M.; Hutri-Kahonen, N.; Lehtimaki, T.; Jokinen, E.; Laitinen, T.; Viikari, J. S.; Raitakari, O. T.; Juonala, M. Early childhood hospitalisation with infection and subclinical atherosclerosis in adulthood: the Cardiovascular Risk in Young Finns Study. *Atherosclerosis* **2015**, *239*, 496-502.

(52) Kozarov, E. Bacterial invasion of vascular cell types: vascular infectology and atherogenesis. *Future Cardiol.* **2012**, *8*, 123-138.

(53) Tong, D.-Y.; Wang, X.-H.; Xu, C.-F.; Yang, Y.-Z.; Xiong, S.-D. Hepatitis B virus infection and coronary atherosclerosis: Results from a population with relatively high prevalence of hepatitis B virus. *World J. Gastroenterol.* **2005**, *11*, 1292-1296.

(54) Galkina, E.; Ley, K. Immune and inflammatory mechanisms of atherosclerosis. *Annu. Rev. Immunol.* **2009**, *27*, 165-197.

(55) Yuan, H.; Zelkha, S.; Burkatovskaya, M.; Gupte, R.; Leeman, S. E.; Amar, S. Pivotal role of NOD2 in inflammatory processes affecting atherosclerosis and periodontal bone loss. *Proc. Natl. Acad. Sci. USA* **2013**, *110*, E5059-5068.

(56) Watanabe, T.; Asano, N.; Murray, P. J.; Ozato, K.; Tailor, P.; Fuss, I. J.; Kitani, A.; Strober, W. Muramyl dipeptide activation of nucleotide-binding oligomerization domain 2 protects mice from experimental colitis. *J. Clin. Invest.* **2008**, *118*, 545-559.

(57) Tang, X. R.; Amar, S. Kavain inhibition of LPS-induced TNF-alpha via ERK/LITAF. *Toxicol. Res.* **2016**, *5*, 188-196.

TABLE OF CONTENTS GRAPHIC